

## **INFORMATION TO USERS**

This manuscript has been reproduced from the microfilm master. UMI films the text directly from the original or copy submitted. Thus, some thesis and dissertation copies are in typewriter face, while others may be from any type of computer printer.

**The quality of this reproduction is dependent upon the quality of the copy submitted.** Broken or indistinct print, colored or poor quality illustrations and photographs, print bleedthrough, substandard margins, and improper alignment can adversely affect reproduction.

In the unlikely event that the author did not send UMI a complete manuscript and there are missing pages, these will be noted. Also, if unauthorized copyright material had to be removed, a note will indicate the deletion.

Oversize materials (e.g., maps, drawings, charts) are reproduced by sectioning the original, beginning at the upper left-hand corner and continuing from left to right in equal sections with small overlaps.

ProQuest Information and Learning  
300 North Zeeb Road, Ann Arbor, MI 48106-1346 USA  
800-521-0600

**UMI<sup>®</sup>**



**Constraints on the Genesis of the  
Archaean Troilus Gold-Copper Deposit, Quebec**

by

**Patricia Carles**

A thesis submitted to the Faculty of  
Graduate Studies and Research in partial  
fulfillment of the requirements for the  
degree of Master of Science

**Department of Earth and Planetary Sciences**

**McGill University, Montreal**

**December 2000**

**© Patricia Carles, 2000**



**National Library  
of Canada**

**Acquisitions and  
Bibliographic Services**

**385 Wellington Street  
Ottawa ON K1A 0N4  
Canada**

**Bibliothèque nationale  
du Canada**

**Acquisitions et  
services bibliographiques**

**385, rue Wellington  
Ottawa ON K1A 0N4  
Canada**

*Your file* *Votre référence*

*Our file* *Notre référence*

**The author has granted a non-exclusive licence allowing the National Library of Canada to reproduce, loan, distribute or sell copies of this thesis in microform, paper or electronic formats.**

**The author retains ownership of the copyright in this thesis. Neither the thesis nor substantial extracts from it may be printed or otherwise reproduced without the author's permission.**

**L'auteur a accordé une licence non exclusive permettant à la Bibliothèque nationale du Canada de reproduire, prêter, distribuer ou vendre des copies de cette thèse sous la forme de microfiche/film, de reproduction sur papier ou sur format électronique.**

**L'auteur conserve la propriété du droit d'auteur qui protège cette thèse. Ni la thèse ni des extraits substantiels de celle-ci ne doivent être imprimés ou autrement reproduits sans son autorisation.**

0-612-70393-2

**Canada**

## **Abstract**

The Troilus gold-copper deposit lies within the northeastern part of the Archaean Frotet-Evans greenstone belt, in the Opatica sub-province of the Superior Province, northern Quebec, and contains total reserves of 51 Mt at 1.08 g/t gold, 0.11 % copper, and 1.4 g/t silver. The largest orebody, Zone 87, has been mined by open pit methods since 1993.

Rocks of the Troilus domain include a coarse- to medium-grained metadiorite, a finer-grained amphibolite, a rock with a brecciated texture and felsic dykes, which crosscut the metadioritic pluton, the amphibolite and the breccia. The amphibolite, breccia, and felsic dykes all locally host ore. The chemical signature of the immobile elements, Ti, Al, Y and Zr, and the REE show that metadiorite, amphibolite and breccia are part of the same calc-alkaline suite. The breccia is a magmatic breccia formed by two separate pulses of magma from the same magmatic source, that underwent slightly different degrees of differentiation. The fragments of the breccia were co-magmatic with the metadiorite while the matrix of the breccia, which was intruded later, was co-magmatic with the amphibolite. The felsic dykes, which are also calc-alkaline, may represent more evolved rocks from the same magma source.

A pre-peak metamorphic potassic alteration event affected all the units, and was most intense in the eastern part of the pit. This alteration is characterized by fine-grained biotite in the mafic units and fine-grained muscovite in the felsic dykes. Relative to the unaltered units, the mica schists resulting from this first

stage of alteration were enriched in potassium, and depleted in sodium and calcium. A second phase of alteration, sericitization, occurred after peak metamorphism, and was localized in high-strain zones. Sericitization was characterized by intense leaching of calcium and sodium, and appreciable addition of potassium. Silica is enriched around the high strain zones, forming a silicified envelope several meters thick.

Two major phases of mineralization, but not developed everywhere to the same degree, have been identified in the Troilus deposit. The first mineralizing event accompanied biotitic alteration, and introduced disseminated gold-copper mineralization. This type of mineralization is mainly hosted in amphibolite and the matrix to the breccia, in a zone bounded by two felsic dykes, whereas it is largely absent from fragments in the breccia, the metadiorite and felsic dykes. The second mineralizing event was associated with sericitization, and is represented by gold-bearing quartz veinlets that crosscut the main foliation.

Previous researchers have proposed a porphyry-type model for the genesis of the Troilus deposit. However, evidence that the breccia unit is not hydrothermal but a product of magma mixing, that the felsic dykes predate mineralization, and that mineralization and associated alteration occurred as two discrete events separated by a major episode of regional metamorphism (amphibolite facies), requires that alternative genetic models for the deposit be considered, such as orogenic gold model.

## **SOMMAIRE**

Le gisement or-cuivre de Troilus est situé dans la partie nord-est de la ceinture de roches vertes archéennes de Frotet-Evans, dans la sous-province Opatica de la Province Supérieure du Québec, et abrite des réserves de 51 Mt à 1,08 g/t d'or, 0,11% de cuivre et 1,4 g/t d'argent. La plus importante zone minéralisée, la Zone 87, est exploitée depuis 1993.

Les roches du domaine de Troilus comprennent un pluton métadioritique, une amphibolite à grains fins, une roche à texture bréchique et des dykes felsiques recoupant le pluton métadioritique, l'amphibolite et la brèche.

La signature chimique des éléments immobiles Ti, Al, Y et Zr, et des terres rares, montre que la métadiorite, l'amphibolite et la brèche font partie du même pluton calc-alkalin. La brèche est une brèche magmatique formée par deux intrusions de magma ayant subi différents degrés de différenciation. Les fragments de la brèche sont issus du même magma que la matrice de la brèche qui est elle-même comagmatique et contemporaine avec l'amphibolite. Les dykes felsiques, qui sont également calc-alkalins, pourraient représenter des roches plus différenciées issues de la même source magmatique.

Une phase d'altération potassique précédant le métamorphisme au faciès amphibolite a affecté toutes les unités et est particulièrement développée dans la partie Est de la fosse. Cette alteration est caractérisée par une biotite à grains fins dans les unités mafiques et une muscovite à grains fins dans les dykes felsiques.

Comparés aux roches non altérées, les schistes biotitiques résultant de ce premier épisode d'altération ont été enrichis en potassium et appauvris en sodium et calcium. Une seconde phase d'altération, une séricitisation, s'est développée dans des zones de déformation intense, ultérieure au métamorphisme régional. Cette séricitisation est caractérisée par un lessivage du calcium et du sodium, et par une importante addition de potassium. Un enrichissement en silice autour des zones de déformation intense forme une enveloppe silicifiée de plusieurs mètres d'épaisseur.

Un premier épisode de minéralisation accompagna l'altération biotitique et introduisit une minéralisation en or et en cuivre, principalement sous forme disséminée. Ce type de minéralisation est restreint aux roches mafiques dans une zone limitée par deux dykes felsiques. Le second épisode de minéralisation est associé à la séricitisation et s'exprime par des veinules de sulfures et de quartz riches en or qui recourent la foliation principale.

De précédentes études ont proposé un modèle génétique de type porphyrique pour la genèse du gisement de Troilus. Cependant, le fait que l'unité bréchique ne soit pas d'origine hydrothermale mais le produit d'un mélange de magmas, que les dykes felsiques précèdent la minéralisation et que la minéralisation et les altérations se sont produites lors de deux épisodes distincts, séparés par un épisode majeur de métamorphisme régional (faciès amphibolite), permet de considérer d'autres modèles génétiques pour le gisement de Troilus.

***To Madeleine Mathieu***

## **ACKNOWLEDGEMENTS**

I am grateful to my thesis supervisors, Dr. A.E. Williams-Jones and Dr. S. Goodman, for their assistance and for their helpful criticisms.

The Inmet Corporation is also given many thanks for their hospitality, assistance and for providing us with complete access to the deposit and the surrounding area.

This thesis benefited from advice and discussions with Professor Wally MacLean and Professor Robert Martin.

Special thanks are given to Mr. Glenn Poirier and Mrs. Leyla Hoosain who provided assistance for electron microprobe analysis and to my officemates K. Ault, A. Chouinard, V. Bodycomb, S. Archibald, O. Grondin and P. Kister for their friendly discussions on technical, theoretical and social aspects.

Very special thanks to Mr. Moe Momayez for his immeasurable support.

Last, but not least, the author wishes to express his deepest affection and gratitude to her parents and sister for their undivided care, interest and encouragement over the years.

## TABLE OF CONTENTS

ABSTRACT .....	ii
SOMMAIRE .....	iv
ACKNOWLEDGEMENTS .....	vii
TABLE OF CONTENTS .....	viii
LIST OF FIGURES .....	x
PREFACE .....	xii
CHAPTER I: INTRODUCTION .....	1
General Statement .....	1
Previous studies .....	4
Objectives and Methodology .....	6
CHAPTER II: REGIONAL GEOLOGY .....	8
Location .....	8
Geology of the Frotet-Evans belt .....	8
Geology of the Frotet-Troilus domain .....	10
The Troilus Group .....	14
CHAPTER III: JOURNAL MANUSCRIPT .....	18
Abstract .....	20
Introduction .....	22
Regional Geology .....	25
Geology of the mine area .....	27
Mineralization .....	31
Petrography of the least altered rocks .....	34
Geochemistry of the precursor lithologies .....	36
Petrography of the altered rocks .....	44
Alteration geochemistry .....	49
Discussion .....	59
Conclusions .....	71
CHAPTER IV: CONCLUSIONS .....	73

<b>REFERENCES .....</b>	<b>76</b>
<b>APPENDIX .....</b>	<b>88</b>
<b>APPENDIX I: Geochemical host rock analysis .....</b>	<b>89</b>
<b>APPENDIX II: Microprobe analysis .....</b>	<b>97</b>

## LIST OF FIGURES

Figure 2.1	Location of the Troilus deposit (modified after Boily, 1995) .....	9
Figure 2.2	Simplified geological map showing the different lithostratigraphic units of the Frotet-Troilus domain, eastern part of the Frotet-Evans greenstone belt (modified after Gosselin, 1996) .....	11
Figure 2.3	Location of the main regional structures of the Frotet-Troilus domain of the Frotet-Evans greenstone belt (modified after Gosselin, 1996) .....	13
Figure 2.4	Lithostratigraphic relationships of the Troilus Group (modified after Gosselin, 1996). For the location of the different sectors, see Figure 2-3 .....	15
Figure 3.1	Location of the Troilus deposit (modified after Boily, 1995) .....	24
Figure 3.2	Simplified geology of the eastern part of the Frotet-Evans greenstone belt (modified after Gosselin, 1996) .....	26
Figure 3.3	Lithostratigraphic column of the Parker and La Fourche sector (modified after Gosselin, 1996) .....	28
Figure 3.4	Simplified geological map of the Troilus domain showing the location of the two main mineralized zones: Zone 87 and Zone J4 ..	30
Figure 3.5	Photograph and photomicrographs showing the mineralogy and textures of the different units encountered in the 87 zone. <b>a.</b> Breccia composed of irregular white fragments and a dark matrix. <b>b.</b> Reflected light photomicrograph showing an electrum grain included in pyrite from a sulfide vein. <b>c.</b> Reflected light photomicrograph showing electrum in fractures within pyrite .....	33
Figure 3.6	Zr vs. Y plot showing the chemical affinity of the different units of the Troilus deposit. The metadiorite, amphibolite, breccia and felsic dykes have calc-alkaline affinity, whereas pillow lavas in the adjacent domain have tholeiitic affinity. Diagram after Pearce and Cann (1973) .....	38

Figure 3.7	Chondrite-normalized rare earth element profiles for the least altered samples from the different units of the Troilus domain. The chondrite values used in normalizing REE are from Nakamura (1974) .....	39
Figure 3.8	A log (Nb/Y) vs. log (Zr/TiO <sub>2</sub> ) plot showing the compositions of the various igneous rock-types of the Troilus deposit. This diagram classifies the mafic rocks as andesite and the felsic dykes as dacite to rhyolite. Diagram after Winchester and Floyd (1977a) .....	41
Figure 3.9	The composition of variably altered host rock samples of the Troilus deposit as a function of TiO <sub>2</sub> and Al <sub>2</sub> O <sub>3</sub> . Lines passing through the origin represent the alteration lines. The bold curve represents the differentiation trendline based on the least altered samples. The point of intersection of an alteration line with a differentiation line represents the Ti and Al concentration of the precursor for a variably altered suite of samples .....	43
Figure 3.10	Chondrite-normalized rare earth element profiles for the samples of fragment and matrix from the breccia and a least altered sample of metadiorite. The chondrite values used in normalizing REE are from Nakamura (1974) .....	45
Figure 3.11	Histogram showing the average relative mass changes for each major mobile element in the different mafic units .....	51
Figure 3.12	Diagrams showing the absolute mass changes of mobile major elements versus the absolute mass changes of silica in the mafic rocks .....	52
Figure 3.13	Histogram showing the average relative mass changes for each major mobile element in the felsic dykes .....	54
Figure 3.14	Diagrams showing the absolute mass changes of mobile major elements versus the absolute mass changes of silica in the felsic dykes .....	55
Figure 3.15	Diagrams showing absolute mass changes of the mobile elements across a high strain zone in a felsic dyke. The degree of deformation increases from the left to the right. The precursor used to monitor the mass changes is on the left of the graphs .....	58
Figure 3.16	Stages in the formation of the breccia. a. Stage 1: intrusion of a metadioritic pluton. b. Stage 2: Fracturing of the outer parts of the pluton due to contraction on cooling. c. Stage 3: intrusion of a second, more mafic, pulse of magma around the pluton and within its fractured outer parts .....	65

## PREFACE

This research was initiated as a collaboration between the author and her supervisors, Professor A. E. Williams Jones and Dr. S. Goodman. The thesis comprises four chapters, one of which is in manuscript format and has been submitted to *Economic Geology*. Collection of the data, petrographic studies and chemical analysis were carried out by the author. Prof. A. E. Williams Jones and Dr. S. Goodman, which provided advice on research methodology, helped evaluating and interpreting the data and critically reviewed the text, are co-authors of the manuscript. The co-authors B. Boily and C. Dion, provided introduction to the geology of the area and important insights about the nature and possible controls of mineralization.

This thesis was written in the form of a journal manuscript, entitled *The Archaean Troilus gold-copper deposit, Chibougamau, Quebec: A product of superimposed pre- and post-metamorphic mineralization*, in accordance with the regulations put forth by the Faculty of Graduate Studies and Research, McGill University. In addition, an introduction, regional geology and concluding chapter were written in order to provide a comprehensive description of the research.

## **CHAPTER I: INTRODUCTION**

### **General statement**

The literature on Archaean gold deposits shows that most of them belong to a coherent genetic group characterized by structurally controlled lode-style mineralization. The deposits are epigenetic and structurally controlled, generally in late, commonly reactivated, shear zones, which have consistent enrichments in gold, variable enrichment of Ag, As and W and only traces of other base metals (Groves, 1993). The gold may occur in any rock type and the deposits range in form from auriferous quartz veins and veinlet systems, disseminated pyritic quartz-albite, potassium feldspar-carbonate replacement zones, and breccias or stockworks (Hodgson, 1993). Pyrite is the dominant sulfide followed by pyrrhotite and arsenopyrite. Evidence from the Yilgarn Block, Western Australia (Groves et al, 1992), and the Abitibi Greenstone belt, Canada (Colvine 1989) indicates that these so-called lode gold deposits represent a crustal continuum that formed under a variety of crustal regimes over a vertical interval of at least a 15 km, at pressure-temperature conditions ranging from 180°C at <1 kb to 700°C at 5 kb (Groves, 1993). Therefore, although most of the lode gold deposits are hosted in greenschist-facies rocks, significant numbers of lode deposits occur in subgreenschist facies and amphibolite or granulite facies rocks. Proximal wall-rock alteration assemblages in the ore zone in mafic-hosted

deposits vary systematically with the metamorphic grade of the enclosing rocks. At greenschist facies the assemblages dolomite/white mica-chlorite or biotite are common, while at low to mid-amphibolite grade amphibole-biotite-plagioclase assemblages are dominant, and give way to diopside-biotite-garnet-K feldspar assemblages at mid-amphibolite to lower granulite grade.

Although lode deposits represent the dominant class of Archaean gold deposits, some recent studies suggest that porphyry-type systems are more common in the Precambrian than generally believed and are widespread in Archaean greenstone belts (Sinclair, 1982; Symons et al, 1988; Sillitoe, 1993). The recognition of these Archaean deposits as porphyry-type was based on the nature of the alteration, the style of mineralization, their common association with felsic dykes contemporaneous with the mineralization and the presence of hydrothermal breccias.

In the idealized porphyry model, alteration in and around the ore deposit is zoned from a potassium-silicate zone at the core, outwards through phyllic, argillic and propylitic zones (Lowell and Guilbert, 1970). The potassium-silicate alteration is the type that is most widely described and perhaps most commonly seen (Tittley, 1993). The bulk of gold in gold-rich porphyry deposits is introduced during this phase of alteration (Sillitoe, 1993), which is characterized by assemblages of biotite, orthoclase, and, in some instances, muscovite or sericite, plus quartz. The propylitic alteration is characterized by the coexistence of chlorite, epidote, calcite and locally albite and is typically synchronous with potassic alteration. Phyllic alteration is characterized by quartz-sericite-pyrite

assemblages, and is typically structurally controlled, occurring as an overprint on earlier potassic alteration (Sillitoe, 1993). The argillic alteration is not always present and consists of quartz, pyrophyllite, and kaolinite. It is most widespread in the upper, volcanic-hosted parts of gold-rich porphyry systems. The nature of the different alteration types varies with the composition of their igneous hosts. In granites and quartz monzonites, potassic alteration is represented by K-feldspar, whereas in diorites, biotite is the principal potassic mineral. The intensity also varies; phyllic and argillic alteration are commonly intense in granite porphyries but weak in diorite porphyries (Hollister, 1978).

In gold-rich porphyry deposits, the mineralization is present in zones of veinlet stockworks and as disseminations within or immediately contiguous to porphyry intrusions (Sillitoe, 1993), and gold and copper concentrations vary sympathetically. The overall grades are low and the tonnage high. Of 29 porphyry gold deposits mentioned in Sillitoe (1993) only 4 have a gold grade > 1 g/t.

Although the porphyry model shares some characteristics with lode-gold deposits, for example the occurrence of potassic alteration and the style of mineralization, other features are very different:

- ◆ Lode-gold deposits are characteristically enriched in gold but rarely in copper and zinc, while the porphyry deposits are polymetallic with enrichment of gold and copper, which vary usually sympathetically.
- ◆ Lode-gold deposits appear to have formed during a regional metamorphic event, most commonly post-peak metamorphism, while

porphyry deposits are related, spatially and temporally, to a magmatic intrusion.

- ◆ Where felsic intrusions are spatially associated with lode-gold mineralization, they typically are not temporally associated.
- ◆ Porphyry-type deposits are commonly associated with hydrothermal breccias, which may carry higher copper and gold contents than surrounding stockwork and disseminated zones.

### **Previous studies**

This research concerns the Archaean Troilus gold-copper deposit, which lies within the northeastern part of the Archaean Frotet-Evans greenstone belt, in the Opatica sub-province of the Superior Province, northern Quebec. The deposit is being exploited by open-pit mining, with present reserves estimated at 51 Mt at 1.08 g/t gold, 0.11 % copper, and 1.4 g/t silver.

Fraser (1993) authored the first published report on the geology of the deposit and proposed, on the basis of similarities between the Troilus deposit and volcanic-porphyry systems, that it represented an Archaean porphyry system, in particular a 'volcanic-porphyry' type as defined by MacMillan and Panteleyev (1980). The specific features noted by Fraser (1993) are the association of the sulfide mineralization with a zoned hydrothermal alteration assemblage, multiple stages of lensoid and anastomosing felsic porphyry

intrusions, a core of chalcopyrite-pyrite-pyrrhotite and a peripheral pyrite-chalcopyrite zone, a mineralized hydrothermal breccia and the disseminated and stringer style of mineralization. Fraser (1993) acknowledged that there are some important differences from more typical porphyry gold systems, notably the high tenor of the gold and its relatively coarse grain size (20-100 microns), and the lack of a magnetite alteration zone.

Magnan (1993) noted the same discrepancies as Fraser (1993), and in addition reported that the chemistry of the alteration minerals is at odds with published data from known porphyry systems. The alteration zoning and presence of sulfide veins and stringers are consistent with the deep-level mesothermal lode-gold model of Robert (1990). However, Magnan (1993) recognized that the lack of important quartz veins, the abundance of gold-rich felsic dykes and the mineralized breccia are features that are atypical of lode-gold deposits. He concluded that the Troilus deposit should be classified with other gold deposits hosted by amphibolite-facies rocks, such as the Hemlo deposit (Kuhns, 1986). Dion et al. (1998) considered the felsic dykes to be contemporaneous with mineralization at  $2782 \pm 6$  Ma, and stressed the volcanic-porphyry model for the deposit.

## **Objectives and methodology**

The main objectives of this research are to characterize, by a combination of mapping, core logging, petrography and geochemistry, the alteration, deformation and mineralization phases and their timing relationships, and thereby provide essential information for constraining genetic models. A subordinate objective is to provide information that could help increase reserves and prolong mine life, or lead to more efficient exploitation of the adjacent mineralized zone (zone J4), which has been evaluated but not yet mined. It is also hoped that the work will contribute to the development of a predictive exploration model that will stimulate exploration for similar deposits in other parts of the Frotet-Evans greenstone belt, which has seen very little exploration work, compared to other greenstone belts in Canada.

In order to describe precisely the geology and metallogeny of the Troilus deposit, sampling, mapping, logging of cores across the area, and compilation of mine assay data were carried out during a three-month period in the field. The laboratory work (microscopic observation of thin sections and microprobe analysis) was necessary to categorize the different mineral parageneses and their crosscutting relationships. Because the original texture of the rock is obscured by superimposition of alteration and metamorphism, primary character was determined from the immobile element geochemistry (elements like Ti, Al, Zr, Nb). Mass changes accompanying alteration and mineralization were

determined by comparing bulk chemical analysis normalized to the concentration of one or more immobile elements.

## **CHAPTER II: GEOLOGY**

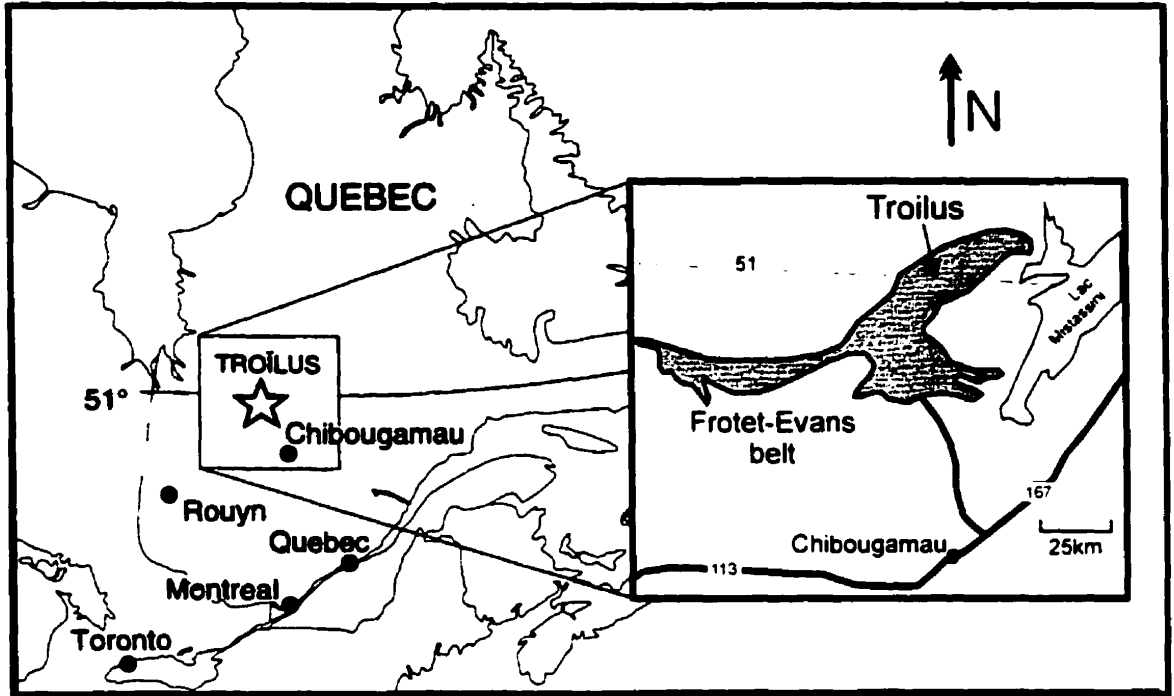
### **Location**

The Troilus gold-copper deposit lies within the northeastern part of the Frotet-Evans greenstone belt, in the Opatica sub-province of the Superior Province, northern Quebec (Fig 2.1).

### **Geology of the Frotet-Evans belt**

The first geological study of the Frotet-Evans greenstone belt was undertaken by Bourne (1973) as part of a regional survey. Gunter (1973, 1977) and Hocq (1974, 1978) mapped the area at a scale of 1:50 000 and produced detailed descriptions of the lithologies encountered. Simard (1982, 1983, 1985, 1987) concentrated on the southern part of the greenstone belt, producing maps at a scale of 1:20 000. He established the lithostratigraphy of the belt, and identified the main trends in the evolution of the volcanic rocks and the main structural domains. Gosselin (1993, 1994) completed the 1:20 000 scale mapping of the belt. A synthesis of the geological surveying of the Frotet-Evans greenstone belt is contained in Gosselin (1996), which summarizes the current state of knowledge of lithostratigraphy, lithogeochemistry, structural geology and economic geology in the area.

**Figure 2.1** Location of the Troilus deposit (modified after Boily, 1995).

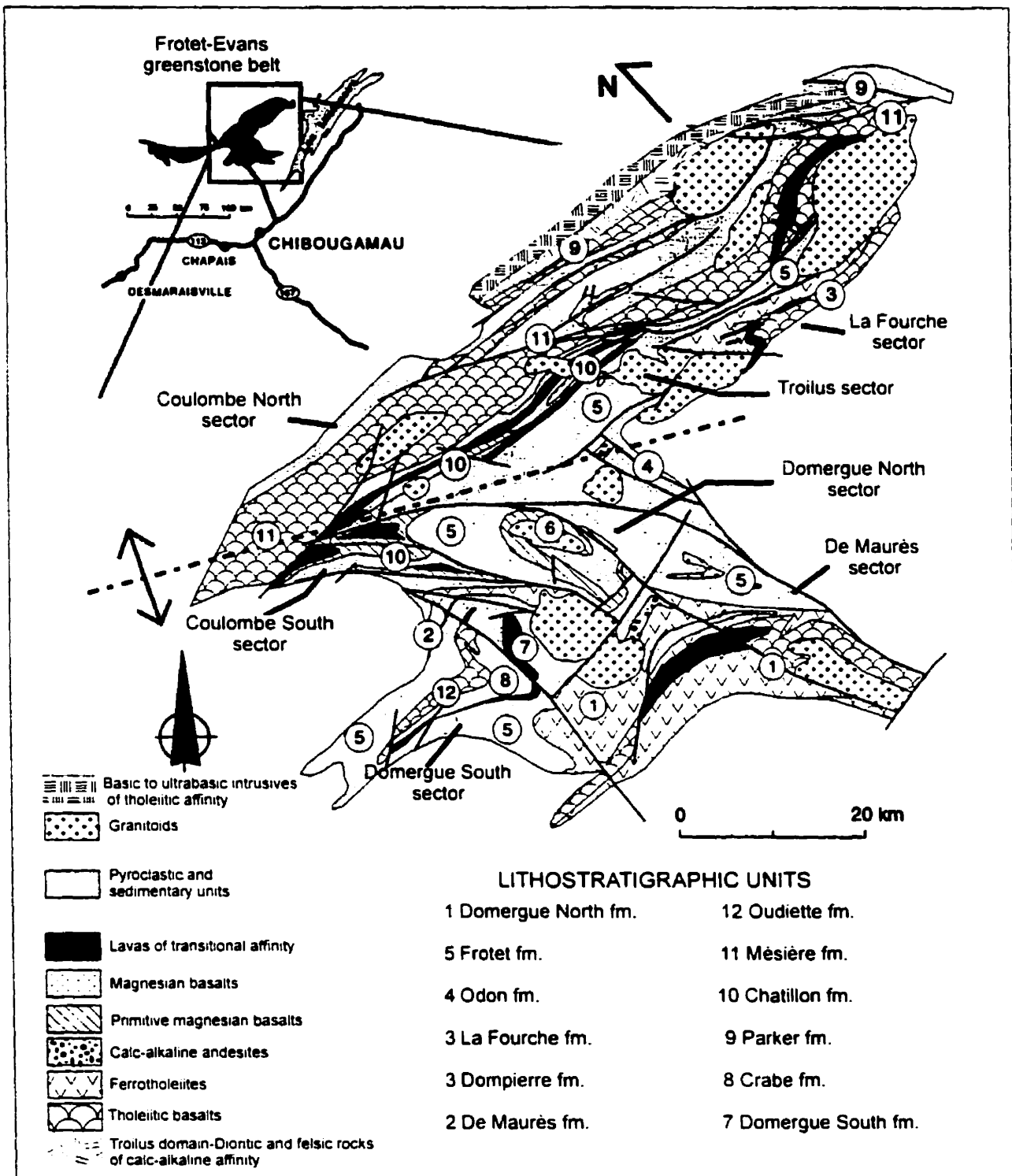


The Frotet-Evans Archean greenstone belt extends for more than 300 kilometers between James Bay and Mistassini Lake, and varies from a few kilometers to 45 km in width. It comprises two similar volcano-sedimentary domains (west domain and east domain). Half of the west volcanic domain is formed of tholeiitic basalts (amphibolites), the remainder being felsic pyroclastic rocks, intrusions of gabbro, pyroxenites and peridotites (Hocq, 1994). The east volcanic domain, which was studied in detail by Simard (1987), is known as the Frotet-Troilus domain.

### **Geology of the Frotet-Troilus domain**

The volcano-sedimentary sequence of the Frotet-Troilus domain is composed of tholeiitic lavas, including basalts with variable magnesium contents and ferro-tholeiites, lavas of transitional affinity, calc-alkaline pyroclastic rocks and sedimentary rocks. Several calc-alkaline andesitic lavas are also present. Variably differentiated sills of ultramafic to granophyric composition are common in some sectors. These intrusives could be comagmatic with the tholeiitic lava units (Simard, 1987). Some porphyritic felsic intrusives are present and could be related to pyroclastic rocks interpreted to be products of explosive volcanism (Gosselin, 1996). A simplified geological map of the Frotet-Troilus domain is presented in figure 2.2.

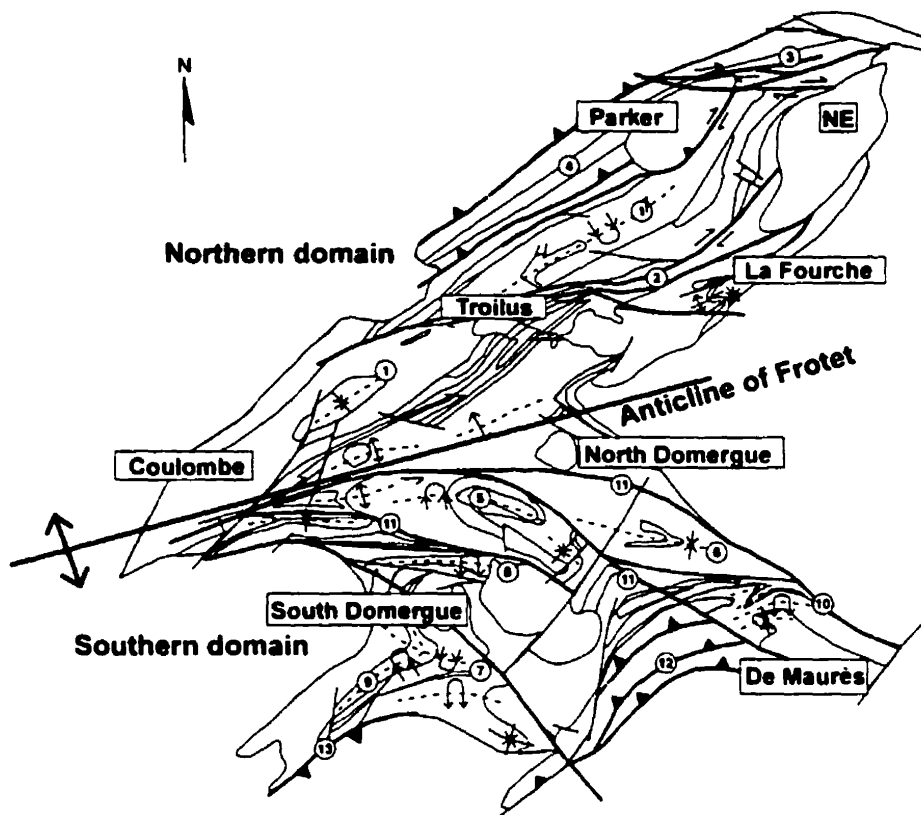
**Figure 2.2** Simplified geological map showing the different lithostratigraphic units of the Frotet-Troilus domain, eastern part of the Frotet-Evans greenstone belt (modified after Gosselin, 1996).



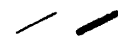
The Frotet antiform divides the terrain into two sub-domains (figure 2.3). The structural features of the northern sub-domain have mainly a dominant NE to ENE trend. In this sub-domain, major structures include the Troilus syncline (Simard, 1987), SE-directed reverse faults, and faults with ENE to EW directed dextral strike slip (Gosselin, 1993, 1994). In the southern sub-domain, the general trend of the major structures is ESE to SE. This sub-domain is characterized by large-scale synclines, the limbs of which are affected by SE to E-W regional-scale faults. Some NE-trending folds and SE-directed reverse faults of regional importance are found near the southern limit of this sub-domain. The main structural features of these sub-domains are presented in figure 2.3.

The regional metamorphic grade of the Frotet-Troilus domain varies from greenschist facies in the internal sectors of the belt to lower amphibolite facies near the felsic intrusives and in a zone a few kilometers wide along the border of the belt (Gosselin, 1996).

**Figure 2.3** Location of the main regional structures of the Frotet-Troilus domain of the Frotet-Evans greenstone belt (modified after Gosselin, 1996).



- 1-Troilus syncline
- 2-La Fourche fault zone
- 3-Dionne fault zone
- 4-Parker fault zone
- 5-Cuvette syncline
- 6-De Maurès syncline
- 7-Crabe syncline
- 8-Dompierre anticline
- 9-Oudiette syncline
- 10-NE directed folds of the De Maurès eastern part
- 11-SE to E-W trending fault zone of the southern sub-domain
- 12-De Maurès reverse faults
- 13-Oudiette fault

 Faults  
 Fold axis

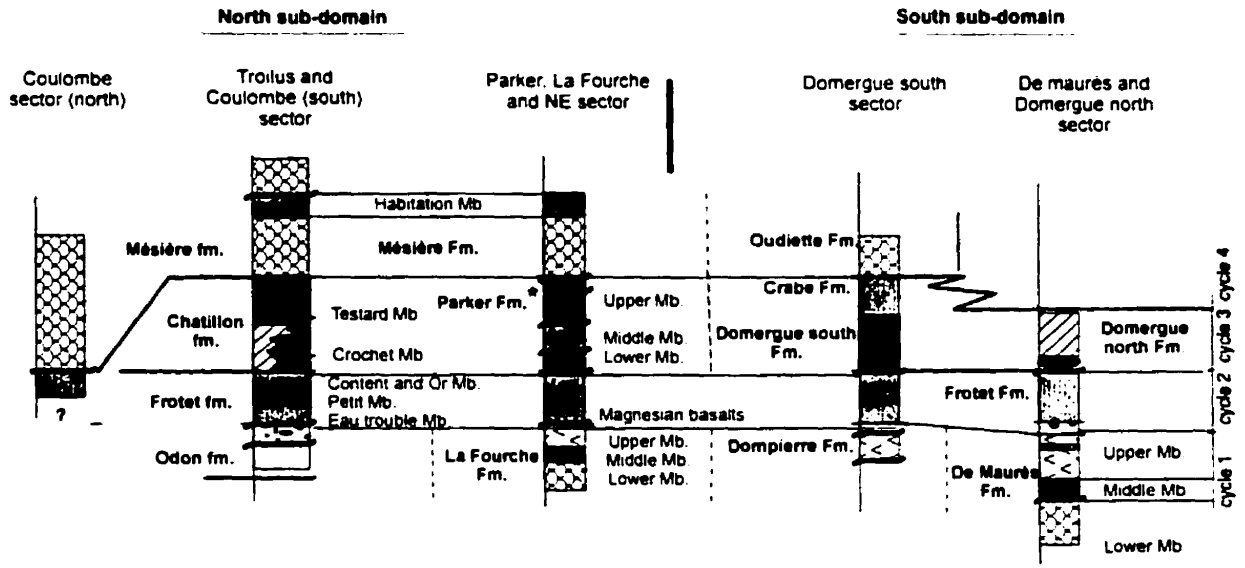
## **THE TROILUS GROUP**

The Troilus deposit is situated just outside the area mapped by Simard (1987) and is hosted by rocks of the Troilus Group. This geological interpretation of the stratigraphy of the Troilus Group is based on his work and that of Gosselin (1996), who studied the lithogeochemistry of the different units in some detail. The Troilus Group was first defined in the Troilus sector (20 km south of the Troilus deposit) by Simard (1983, 1987). The different lithologies of the Troilus Group and their regional stratigraphic relations are shown in the stratigraphic column presented in figure 2.4. The lithologies hosting the Troilus deposit and immediately adjacent to it are described below.

The oldest formation, La Fourche, is composed of a sequence of deformed and amphibolitized massive and layered pillow-lavas. These locally contain quartz-carbonate amygdules and are interbedded with thin layers of felsic to intermediate tuffs, metapelite, and graphitic schists. Based on chemical compositions, Gosselin (1996) divided the formation in three members:

- ◆ a lower Member, composed of tholeiitic basalts
- ◆ a middle Member, composed of lavas of transitional affinity.
- ◆ an upper Member, composed of highly differentiated ferro-tholeiites.

**Figure 2.4** Lithostratigraphic relationships of the Troilus Group (modified after Gosselin, 1996). For the location of the different sectors, see Figure 2-3.



- |  |   |  |   |  |  |
|--|---|--|---|--|--|
|  | Undifferentiated pyroclastic or sedimentary units |  | Ferro-tholeites   |  | Uncertain stratigraphic limit because of an insufficient geological control                          |
|  | Andesites of calc-alkaline affinity               |  | Tholeiitic basalts  |  | Komatiitic basalts   |
|  | Magnesian basalts                                 |  | Primitive tholeiitic magnesian basalts with minor proportions of transitional lavas and pyroclastic and sedimentary rocks |  | Units of lavas of transitional affinity interstratified with volcanoclastites in variable proportion |
|  |   |  |   |  | Stratigraphic position of the Troilus deposit  |

The Frotet Formation stratigraphically overlies the La Fourche Formation and occupies the core of the Frotet Lake anticline. It consists of a thick sequence of fine to coarse intermediate composition pyroclastic rocks, predominantly lapilli and crystal tuffs of calc-alkaline affinity. The lower Member is the Eau Trouble Member, composed of porphyritic and felsic tuffs. Overlying the Eau Trouble Member are the Petit Member (crystal tuffs), the Content Member (leucocratic tuffs with minor fine-grained sedimentary rocks) and the Or Member (felsic lavas with phenocrysts of plagioclase).

The Parker Formation is sub-divided in three members:

- ◆ The lower Member is composed of mafic rocks (gabbro or lavas) of transitional affinity, and volcanoclastic rocks of intermediate to felsic composition.
- ◆ The middle Member consists of massive metavolcanoclastic rocks.
- ◆ The upper Member comprises pillowed or brecciated andesites and basalts of transitional to calc-alkaline affinity. These lavas locally contain garnets, in horizons several meters thick. Felsic to intermediate tuff beds a few meters thick are common within the lavas.

The Mésière Formation, volumetrically the most important unit in the Troilus Group, consists of tholeiitic pillow basalts with thin interbeds of intermediate to felsic tuffs. The basalts have a very homogeneous chemical composition and have a tholeiitic affinity.

At the top of the Troilus Group, the Habitation Member is composed of pyroclastic rocks of calc-alkaline affinity and sedimentary rock. This unit occupies

the center of the Troilus Lake syncline. It is composed of crystal tuffs with plagioclase and quartz fragments at the base of the sequence. Locally bedded, this deposit could be epiclastic. The uppermost part of the member is composed of crystal tuffs, lapilli tuffs, leucocratic tuffs, and argillaceous sediments.

The Troilus deposit lies within a calc-alkaline domain, at the stratigraphic level of the Parker Formation. Calc-alkaline rocks of the Troilus domain include a coarse- to medium-grained metadiorite, a finer-grained amphibolite, a rock with a brecciated texture and felsic dykes, which crosscut the metadioritic pluton, the amphibolite and the breccia. A few late tholeiitic mafic dykes and pegmatitic dykes crosscut the calc-alkaline units.

**CHAPTER III:  
JOURNAL MANUSCRIPT**

**The Archaean Troilus gold-copper deposit, Chibougamau, Quebec: A product  
of superimposed pre- and post-metamorphic mineralization.**

**P. Carles, S. Goodman, A.E. Williams-Jones**

*Department of Earth and Planetary Sciences, McGill University, 3450 University Street, Montreal,  
Quebec, Canada H3A 2A7*

**B. Boily**

*Inmet Mining Corporation, Exploration division, 1300 boul. Saguenay, Suite 200  
Rouyn-Noranda, Quebec, Canada J9X 7C3*

**C. Dion**

*Service géologique du Nord-Ouest, Géologie Québec  
400, Boul. Lamaque, Bur. 1.02 Val-d'Or, Quebec, Canada J9P 3L4*

## **Abstract**

The Troilus gold-copper deposit lies within the northeastern part of the Archaean Frotet-Evans greenstone belt, in the Opatica sub-province of the Superior Province, northern Quebec, and contains total reserves of 51 Mt at 1.08 g/t gold, 0.11 % copper, and 1.4 g/t silver. The largest orebody, Zone 87, has been mined by open pit methods since 1993.

Rocks of the Troilus domain include a coarse- to medium-grained metadiorite, a finer-grained amphibolite, a rock with a brecciated texture and felsic dykes, which crosscut the metadioritic pluton, the amphibolite and the breccia. The amphibolite, breccia, and felsic dykes all locally form ore. The chemical signature of the immobile elements, Ti, Al, Y and Zr, and the REE show that metadiorite, amphibolite and breccia are part of the same calc-alkaline suite. The breccia is a magmatic breccia formed by two separate pulses of magma, that underwent slightly different degrees of differentiation. The fragments of the breccia were co-magmatic with the metadiorite while the matrix of the breccia, which was intruded later, was co-magmatic with the amphibolite. The felsic dykes, which are also calc-alkaline, may represent more evolved rocks from the same magma source.

A pre-peak metamorphic potassic alteration event affected all the units, and was most intense in the eastern part of the pit. This alteration is characterized by fine-grained biotite in the mafic units and fine-grained muscovite in the felsic dykes. Relative to the unaltered units, the mica schists resulting from this first stage of alteration were enriched in potassium and iron, and depleted in sodium and calcium.

A second phase of alteration, sericitization, occurred after peak metamorphism, and was localized in high-strain zones. Sericitization was characterized by intense leaching of calcium and sodium, and appreciable addition of potassium. Silica is enriched around the high strain zones, forming a silicified envelope several meters thick.

Two major phases of mineralization, but not developed everywhere to the same degree, have been identified in the Troilus deposit. The first mineralizing event accompanied biotitic alteration, and introduced disseminated gold-copper mineralization. This type of mineralization is mainly hosted in amphibolite and the matrix to the breccia, in a zone bounded by two felsic dykes, whereas it is largely absent from fragments in the breccia, the metadiorite and felsic dykes. The second mineralizing event was associated with sericitization, and is represented by gold-bearing quartz veinlets that crosscut the main foliation.

Previous researchers have proposed a porphyry-type model for the genesis of the Troilus deposit. However, evidence that the breccia unit is not hydrothermal but a product of magma mixing, that the felsic dykes predate mineralization, and that mineralization and associated alteration occurred as two discrete events separated by a major episode of regional metamorphism (amphibolite facies), requires that alternative genetic models for the deposit be considered.

## Introduction

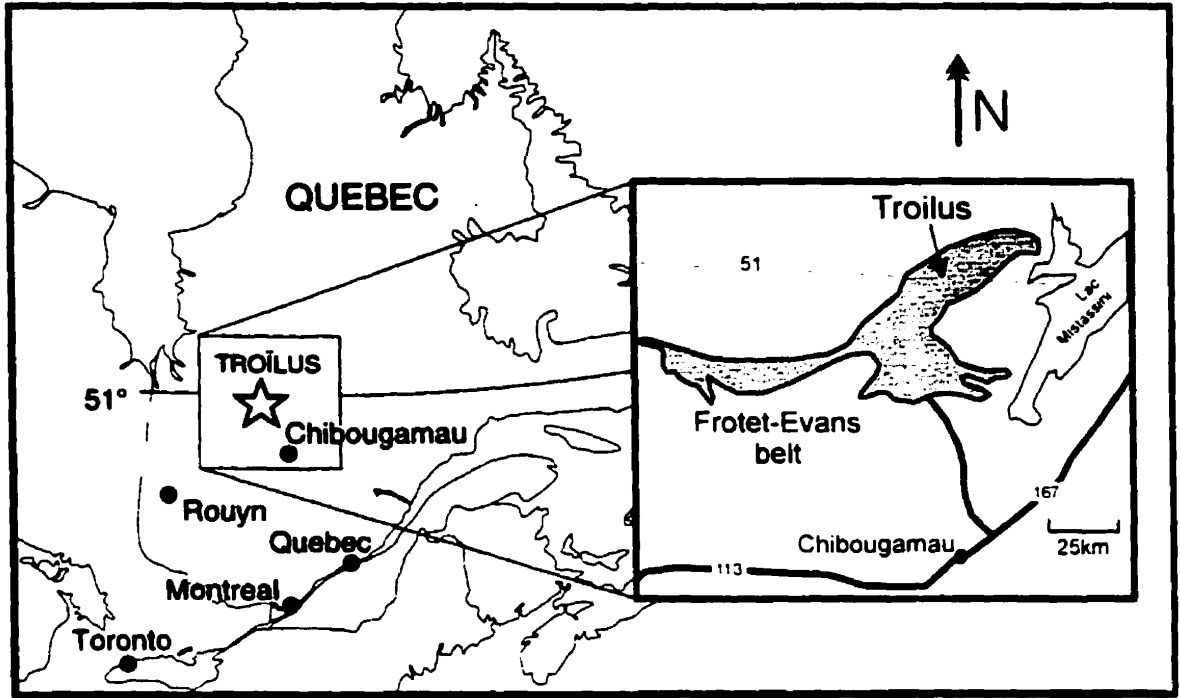
A knowledge of the geochemical changes associated with ore-related hydrothermal alteration is an important starting point for determining the composition of the hydrothermal fluid and the physico-chemical controls of mineralization. Moreover, the spatial variation of such alteration (zonation) may provide a vector towards ore in exploration programmes. However, when a rock unit is altered and metamorphosed, its mineralogical, textural and chemical characteristics are changed to such a degree that its primary nature may be unrecognizable (Whitford et al, 1989; Barrett and MacLean, 1991). This is commonly the case for rocks hosting mineral deposits, particularly when the grade of metamorphism reaches amphibolite facies or higher (Richardson et al., 1986, MacLean and Hoy, 1991; Shriver and MacLean, 1993). Fortunately, a number of elements commonly found in rock-forming minerals, notably Al, Ti, Nb, and Zr, are immobile under most conditions of alteration and metamorphism (MacLean and Kranidiotis, 1987), and their ratios may therefore be used to determine the primary nature of the rocks and the chemical changes that have affected them. In this study, we make use of immobile element techniques (Pearce and Cann, 1973; Winchester and Floyd, 1977(a); Winchester and Floyd, 1977(b), MacLean, 1990, MacLean and Barrett, 1993) to identify the precursors to the amphibolite and breccia hosting mineralization in the Troilus gold-copper deposit, and to evaluate the chemical changes accompanying the different alteration and mineralization events.

The Troilus deposit lies within the northeastern part of the Archaean Frotet-Evans greenstone belt, in the Opatica sub-province of the Superior Province, northern Quebec (Fig. 3.1), and contains total reserves of 51 million metric tonnes of ore at 1.08 g/t gold, 0.11 % copper, and 1.4 g/t silver, in two main ore zones (zone 87 and zone J4). The deposit is being exploited by open-pit mining of the 87 zone.

Fraser (1993) proposed that the deposit is of porphyry-type based on similarities to subvolcanic-porphyry ore-forming hydrothermal systems. Some of these similarities are said to be an association of the sulfide mineralization with a zoned hydrothermal alteration assemblage, multiple stages of lensoid and anastomosing felsic porphyry intrusions, a core of chalcopyrite-pyrite-pyrrhotite and a peripheral pyrite-chalcopyrite zone, and the disseminated and stringer style of mineralization. However, Fraser (1993) acknowledged some important differences from more typical porphyry-gold systems, such as the relatively coarse gold grain size (20-100 microns), the high tenor of gold, the lack of a magnetite alteration zone and the presence of strong sodic alteration. According to Magnan (1993) the alteration zoning and presence of sulfide veins and stringers are consistent with the deep-level mesothermal lode-gold model of Robert (1990). However, he could not explain the lack of mesoscopic/macroscopic quartz veins, the abundance of gold-rich felsic dykes and the occurrence of mineralized breccia. Magnan (1993) recommended that the Troilus deposit should be classified with other gold deposits hosted by amphibolite-facies rocks, such as the Hemlo deposit (Kuhns, 1986).

The exposure in the open pit and an extensive geological database from drill

**Figure 3.1** Location of the Troilus deposit (modified after Boily, 1995)



holes has provided the means to advance significantly our understanding of the controls of mineralization. This paper reports the results of a geochemical study of the different units of the deposit, viewed in conjunction with field relationships and alteration mineralogy. The original composition of the host rocks has been determined, and the chemical changes accompanying alteration and mineralization evaluated quantitatively. This has yielded more extensive and detailed information on the alteration, deformation and mineralization and therefore has permitted greater constraint to be placed on genetic modeling.

### **Regional Geology**

Syntheses of the geology of the Frotet-Evans greenstone belt are contained in Simard (1987), Gosselin (1996) and Boily (1998). The belt is underlain by a supracrustal sequence of submarine mafic volcanics with intercalated cogenetic mafic intrusions (Fig. 3.2). Felsic volcanic and pyroclastic rocks and minor epiclastic sedimentary rocks as well as ultramafic horizons are also present. These supracrustal rocks are intruded by granitoid plutons and dykes, which range from pre-tectonic to post-tectonic in age. All the rocks of the belt, except for late granitoid plutons and dykes, are variably deformed. The outcropping rocks strike NE-SW, dip moderately steeply to the NW and are present as a number of SE-directed thrust slices. They generally show a strong planar foliation, however the deformation appears to be localized, with some units showing very little deformation.

**Figure 3.2** Simplified geology of the eastern part of the Frotet-Evans greenstone belt (modified after Gosselin, 1996).

Subhorizontal to megascopic folds are locally common, and affect both the regional foliation and primary layering.

The Troilus deposit lies within a calc-alkaline domain, at the stratigraphic level of the median member of the Parker formation (Gosselin, 1996), which elsewhere is composed mainly of transitional lavas and pyroclastic units (Fig. 3.3). The metamorphic grade in the Frotet-Evans greenstone belt ranges from greenschist to lower amphibolite facies. Thermobarometric investigation of mafic rocks in the mine area yielded pressure and temperature estimates of 6 kbars and 650 °C, respectively (Goodman, 2000).

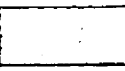
Results of most of the exploration work in the Frotet-Evans greenstone belt remain in company records. However some information is available to the public in assessment reports on open file at the Ministère des Ressources Naturelles du Québec (MRNQ), Val d'Or, Québec (e.g. Palmer, 1973). The largest gold occurrence in the belt is the Troilus deposit. There are also three subeconomic volcanogenic massive sulfide deposits containing copper, zinc, silver, gold and lead (Boily, 1998).

### **Geology of the mine area**

There is very little outcrop in the Troilus domain, and none in the vicinity of the deposit. The geology was therefore reconstructed from drill core, from core logs, and from temporary exposures within the open pit. Owing to the effects of alteration and

**Figure 3.3** Lithostratigraphic column of the Parker and La Fourche sector  
(modified after Gosselin, 1996).

**Parker, La Fourche  
and NE sector**

**Habitation Mb.** 

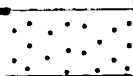
**Mésièrè Fm.**

  **Upper Mb.**

**Parker Fm.**  **Troilus Domain**

  **Lower Mb.**

**Frotet Fm.**

  **Superior Mb.**

**La Fourche Fm.**  **Median Mb.**

**Inferior Mb.**



**Legend**

 Dioritic and felsic rocks of calc-alkaline affinity

 Tholeiitic basalts

 Undifferentiated pyroclastic or sedimentary units

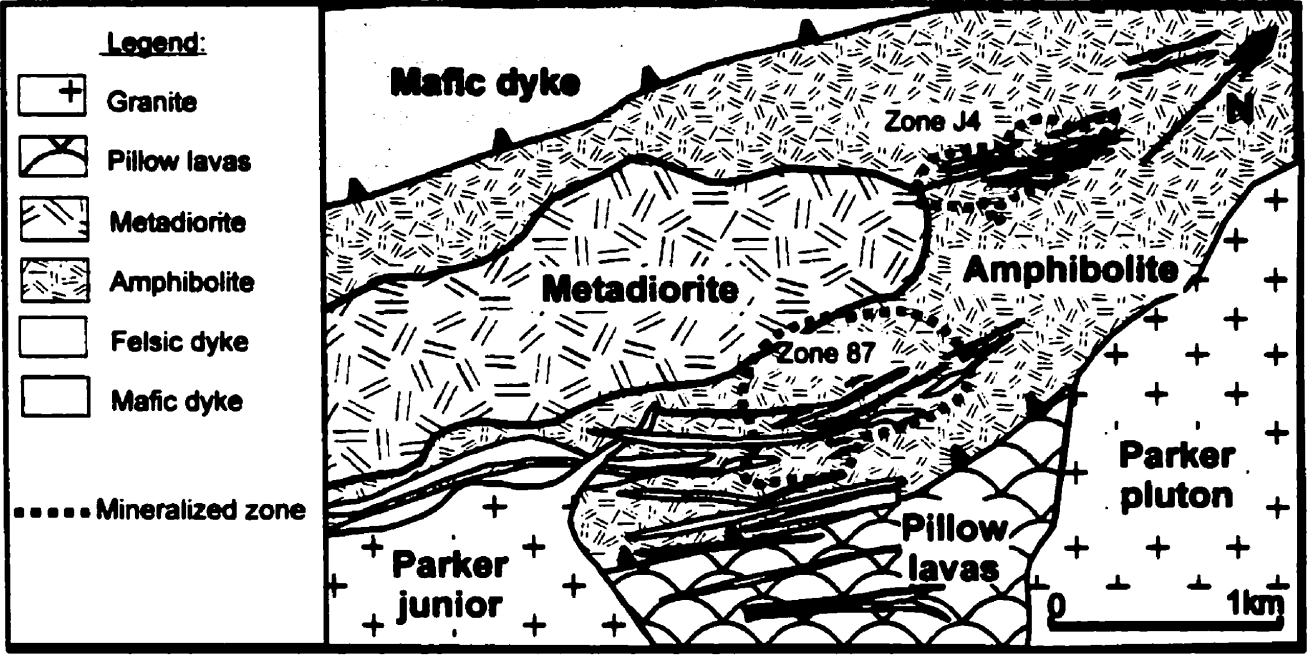
 Units of lavas of transitional affinity interstratified with variable proportions of volcanoclastites

 Ferrotholeiites

regional metamorphism, most rocks retain few if any primary igneous textures, and consequently their original nature is difficult to determine. In the region of the deposit, the Troilus domain comprises a metadioritic pluton (Fig. 3.4, Fig. 3.8) surrounded by a finer-grained amphibolite. In some places, within and around the margins of the pluton, the rock has a brecciated texture, with pale fragments set in a dark amphibolitic matrix (Fig. 3.5a). There are substantial variations in the diameter of fragments, from 1 cm to over 10 cm, in their shape, from equidimensional to highly elongated, and in the colour, from gray to white. The contact between the metadiorite and the amphibolite is underlined by deformed zones over a few centimeters wide, where the metadiorite becomes more foliated and fine-grained. Felsic dykes, 1 m to 20 m wide, crosscut the metadiorite, amphibolite and breccia. A large felsic dyke, which occurs in the footwall of the deposit and is parallel to the main foliation, was dated using the U-Pb method on zircon, and yielded an age of  $2782 \pm 6$  Ma (Pilote et al., 1997). Amphibolite, breccia and felsic dykes are the main hosts to ore in the deposit.

A small number of dark gray to blue-black mafic dykes, ranging from 50 cm to 3 m in width cut all previous rock types and are oblique to the main foliation. They are weakly foliated and metamorphosed to amphibolite. In contrast to the other units, which are calc-alkaline, the mafic dykes have a tholeiitic affinity, as do the barren pillow lavas present to the south of the Troilus domain (Fig. 3.6). The contact between the pillow lavas and the amphibolite is tectonic i.e., it is delineated by zones of deformation. The Parker and the Parker junior granite bodies (Fig. 3.4) are two barren, non-foliated plutons, which are located to the south of the mineralized zones,

**Figure 3.4** Simplified geological map of the Troilus domain showing the location of the two main mineralized zones: Zone 87 and Zone J4.



and cut the southern margin of the Troilus domain. An age of  $2698 \pm 2$  Ma was obtained for the Parker pluton from U-Pb isotopic analysis of magmatic titanite (David, 1999), supporting field observations that it was intruded long after alteration and deformation of the host sequence.

### **Mineralization**

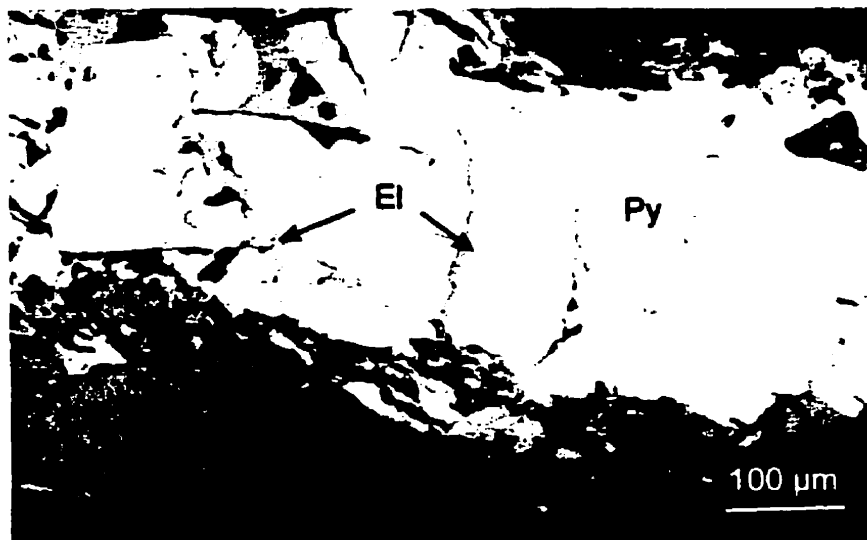
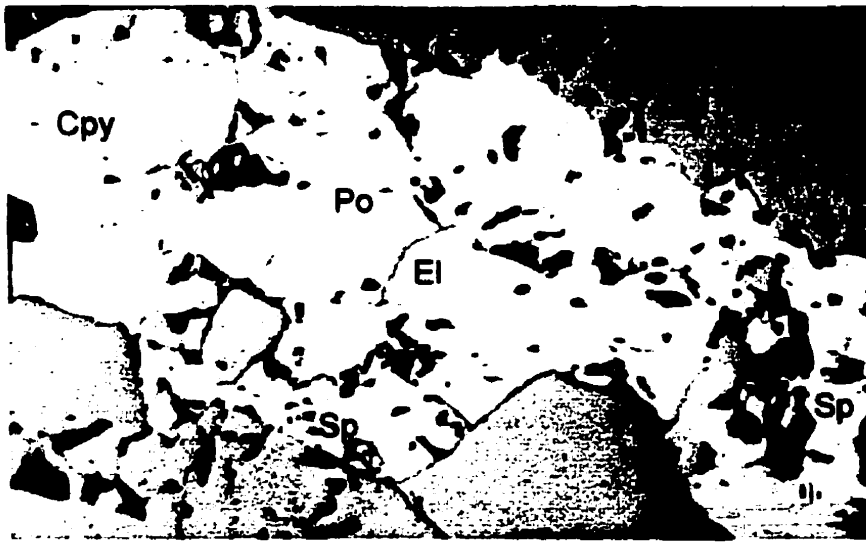
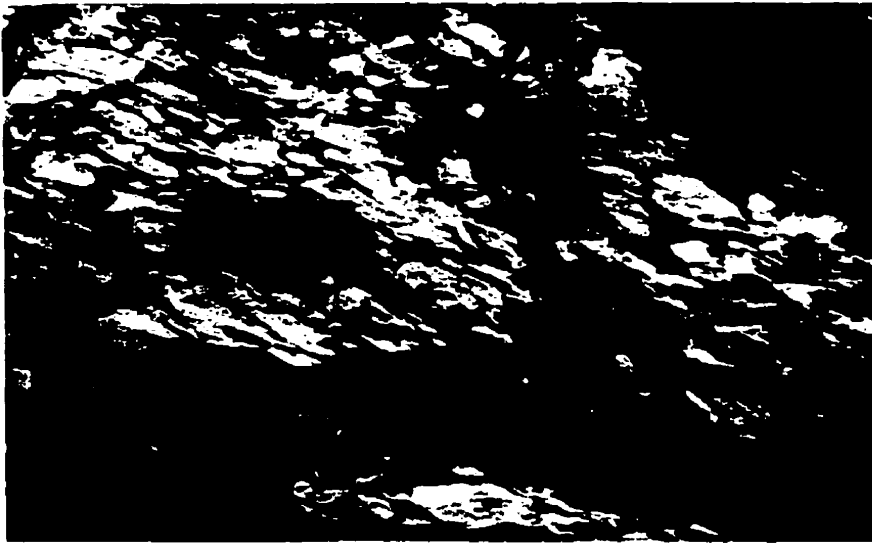
Several mineralized zones occur in the Troilus domain, however our study was restricted to the 87 zone, the orebody which is currently under exploitation. An evaluation of mine assay data indicates that there is a strong correlation of copper with silver but relatively poor correlations between copper and gold, and gold and silver. These data are consistent with the superimposition of two different styles of mineralization: a copper-gold-silver mineralization and a gold- only mineralization, which were first recognized during the course of this study.

The copper-gold-silver mineralization is restricted to amphibolite and to the matrix of the breccia; only the felsic dyke margins, in contact with mineralized rocks of this zone, are mineralized. Based on geochemical data from drill cores, the gold, copper and silver grades increase with the amount of biotite present in the rocks (stage 1 alteration; see below). The metadiorite, the fragments of the breccia, and the biotite-free amphibolite, which are only slightly affected by the potassic alteration, are not mineralized. This copper-gold-silver mineralization comprises pyrite, chalcopyrite and pyrrhotite as small disseminated grains (1 to 5 % of the rock)

and millimeter wide streaks and stringers parallel to the main foliation. Gold is rarely observed in this style of mineralization, but has been reported as fine grains of electrum up to 20  $\mu\text{m}$  wide along sulfide grain boundaries (Carson, 1990). Negligible amounts of invisible gold are present within the sulfides.

The gold-only mineralization is related to sericitization within high strain zones in the felsic dykes, amphibolite and breccia. This style of mineralization is characterized by sporadic high gold grades (up to 100 g/t of gold over 1 m from core assays), and erratic and negligible copper grades. The gold mineralization is restricted to quartz veinlets and veins, which crosscut the main foliation, defined by the biotite, at a slight angle. The veins can be up to 1 cm wide and are more common within a silicified envelope, which surrounds the most highly deformed and sericitized part of the rock. The quartz veins commonly contain variable amounts of muscovite, tourmaline, coarse biotite, chlorite, and minor sulfides (chalcopyrite, pyrite, pyrrhotite, sphalerite and minor galena). For the sulfides, the paragenetic sequence is early pyrite, followed by chalcopyrite with pyrrhotite, and later sphalerite and galena. Gold is found in fractured pyrite grains, along sulfide grain boundaries (particularly pyrrhotite-sphalerite contacts), or as free gold in portions of the veinlets that are sulfide-poor. Gold is most commonly found as electrum (~70% Au and 30% Ag) when in contact with sulfides. (Fig. 3.5b and Fig. 3.5c). Native gold (> 86% Au) occurs in sulfide-poor millimeter wide quartz-muscovite-biotite veinlets, locally in association with tellurobismutite, chalcopyrite, and minor pyrrhotite and pyrite.

Figure 3.5 Photograph and photomicrographs showing the mineralogy and textures of the different units encountered in the 87 zone. **a.** Breccia composed of irregular white fragments and a dark matrix. **b.** Reflected light photomicrograph showing an electrum grain included in pyrite from a sulfide vein. **c.** Reflected light photomicrograph showing electrum in fractures within pyrite.



## **Petrography of the least altered rocks**

A detailed petrographic study was performed on a suite of samples collected in the 87 zone in order to characterize the different units macroscopically and microscopically.

*Metadiorite:* The metadiorite is a mid to dark gray to green medium-grained rock, which forms a pluton located to the west of the mineralized zone (Fig. 3.4). It retains a relict igneous texture despite the grade of metamorphism. Where fresh, it consists of subhedral to euhedral plagioclase and hornblende phenocrysts in a groundmass of plagioclase, amphibole, epidote and quartz with a trace of disseminated pyrite and minor titanite. This pluton is largely unexposed and its contacts with the adjacent amphibolite and breccia are inferred from drill intersections.

*Amphibolite:* Outside the main ore zone, the amphibolite is a dark gray-green to black, fine-grained rock, which is massive to poorly foliated. The principal minerals are actinolitic hornblende, granular epidote and fine-grained quartz and feldspar (10% plagioclase, <5% K-feldspar). These minerals have an allotriomorphic texture and display no obvious evidence of foliation. Ghost-like albite porphyroblasts are commonly present. These are altered to muscovite and calcite, associated with coarser quartz grains and locally surrounded by chlorite. Their proportion varies from 0 to 30%, and their diameter from 0.5 to 2 mm. Commonly, the plagioclase phenocrysts are pseudomorphed by aggregates of quartz and albite. Pyrite and

chalcopyrite (< 1%) and minor sphalerite, titanite and tourmaline are also commonly present.

*Breccia:* Breccia occurs in the hangingwall and footwall of the deposit as well as in the main mineralized zone where it hosts ore (Fig. 3.5a). Outside the main ore zone, the fragments are unfoliated and comprise a fine groundmass of quartz and feldspar enclosing plagioclase phenocrysts, ragged amphibole, pink titanite, needles of epidote and minor calcite. The plagioclase phenocrysts represent 10 to 30% of the fragments, are tabular and range in diameter from 0.5 to 2 mm. Some plagioclase phenocrysts have a preferred orientation and locally are polygonized as a result of the stress suffered by the rock. The matrix to the breccia is poorly foliated and is composed of poikiloblastic hornblende, representing 50% of the material, quartz, plagioclase, zoisite, and biotite. The biotite occurs as fine grains disseminated between quartz and plagioclase in the groundmass or as coarse grains associated with a second generation of idiomorphic epidote.

*Felsic dykes:* The contacts of the felsic dykes with the mafic rocks are generally parallel to the foliation. The felsic dykes are composed of a very fine-grained groundmass of quartz and plagioclase (80% in total) with interspersed lepidoblastic muscovite (15%) and minor biotite and disseminated pyrite. There is no clear evidence of penetrative foliation, although locally small oriented flakes of biotite (5%) define a weak foliation. There are some augen-shaped plagioclase grains (0 to 5%) altered to sericite-epidote, along with muscovite, quartz and calcite. Some dykes have a polygonal pattern of dark millimeter-wide joints, which commonly carry sulfide grains. The joints have a slightly coarser grain than the rest of the rock, and,

in addition to quartz, muscovite and calcite, they contain chlorite, blue-green tourmaline and, in some places, euhedral pyrite with interstitial chalcopyrite and minor sphalerite.

## **Geochemistry of the precursor lithologies**

### *Analytical techniques*

Representative samples were analyzed for major and trace element compositions at the Centre de Recherche Minérale (CRM). All samples were analyzed by X-ray fluorescence (XRF) spectrometry techniques for the major elements as well as for Rb, Ga, Nb, Sr, Y and Zr. Additional analyses were made available by INMET. The concentrations of rare-earth elements and other trace elements were determined by instrumental neutron activation analysis (INAA).

### *Data interpretation*

The first application of the bulk rock geochemical data was to characterize the different lithologies of the Troilus domain by determining their magmatic affinities and identifying the rock-types present. In order to do this, it was first necessary to correct for the effects of hydrothermal alteration. Compositional features of the rocks are illustrated in Figures 3.6-3.9. The elements Al, Ti, Zr, Nb, Y and the REE were used in various combinations to interpret the primary chemistry of the altered magmatic rocks. These elements are potentially the most immobile in rocks

subjected to low-grade metamorphism and hydrothermal alteration (e.g., Pearce and Cann, 1973; Winchester and Floyd, 1977(b)). During hydrothermal alteration, because of changes in the overall mass or volume of the rocks, the concentrations of immobile elements vary but their ratios remain constant. Therefore, a pair of immobile elements can be used to establish affinities of altered rocks. In the geochemical diagrams (Fig. 3.6 to Fig. 3.10), samples have been subdivided according to petrographic designation.

#### *Magmatic affinities*

The magmatic affinities of the different mafic units were determined from a Y-Zr plot (Fig. 3.6) and chondrite-normalized REE profiles (Fig. 3.7). The Zr/Y ratio ranges from ~3 to 5 for tholeiites, from 5 to 7 for transitional rocks and from 7 to 30 for calc-alkaline rocks (Lesher et al., 1986). On this graph (Fig. 3.6), the compositions of metadiorite, amphibolite and breccia cluster between the calc-alkaline and transitional fields, suggesting that they have essentially the same magmatic affinity. The compositions of the felsic dykes also plot in the calc-alkaline to transitional fields, but the concentrations of Y and Zr differ significantly from those of the mafic rocks, as the dykes are more differentiated. The fact that they do not cluster as well on the Y-Zr graph as the mafic rocks can be explained by the fact that Zr and Y become compatible in evolved calc-alkaline magmas (Watson and Harrison, 1983). Their chemical affinity and the close spatial association with the mafic rocks suggest that the felsic dykes could come from the same magmatic source, though this is by no means certain.

**Figure 3.6** Zr vs. Y plot showing the chemical affinity of the different units of the Troilus deposit. The metadiorite, amphibolite, breccia and felsic dykes have calc-alkaline affinity, whereas pillow lavas in the adjacent domain have tholeiitic affinity. Diagram after Pearce and Cann (1973).

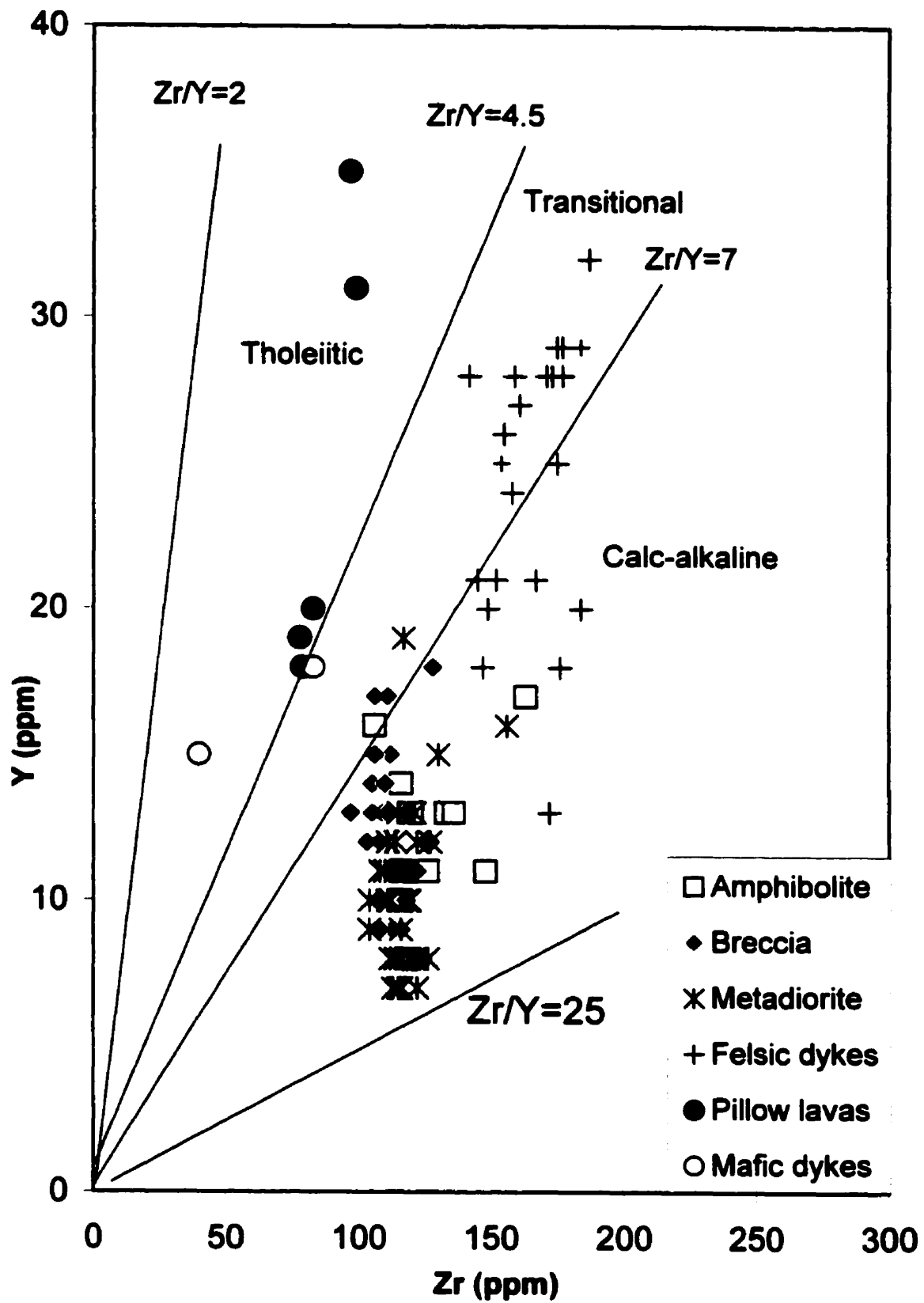
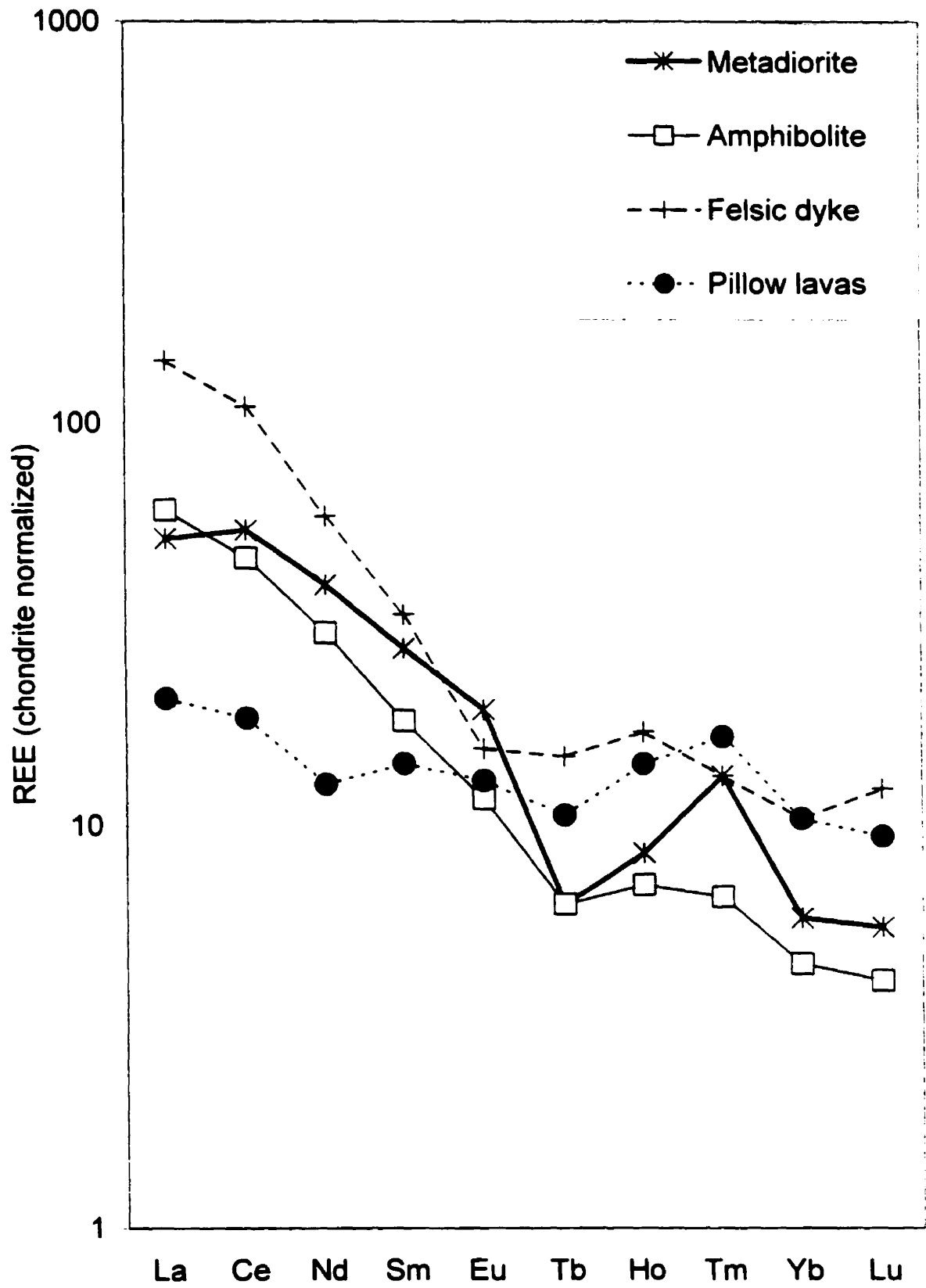


**Figure 3.7** Chondrite-normalized rare earth element profiles for the least altered samples from the different units of the Troilus domain. The chondrite values used in normalizing REE are from Nakamura (1974).



The pillow lavas to the SE of the Troilus domain and the mafic dykes within the pit have a Y/Zr ratio consistent with a tholeiitic affinity, and clearly represent a magmatic event separate from that responsible for the other lithologies. The mafic dykes may represent feeder dykes to the pillow lavas, and, as they crosscut the other lithologies, this magmatic event postdates the calc-alkaline magmatism. Magmatic affinities of the rocks are confirmed by the chondrite-normalized REE profiles of fresh samples (Fig. 3.7). The metadiorite and the amphibolite are enriched in light-REE, and have chondrite-normalized profiles typical of calc-alkaline magmas, whereas the pillow lavas have the relatively flat profiles typical of tholeiitic magmas (Wilson, 1989).

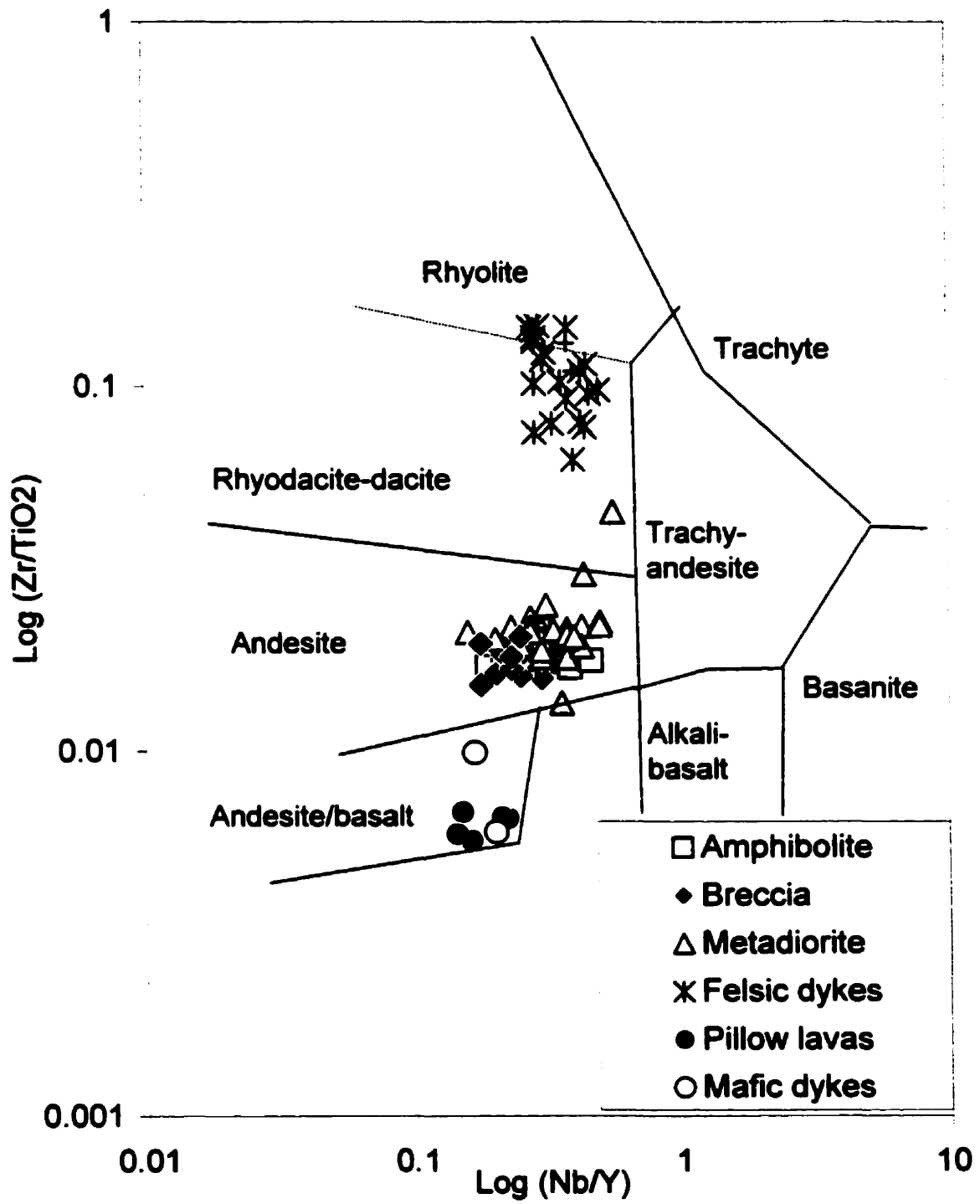
#### *Rock types*

The Nb/Y vs Zr/TiO<sub>2</sub> plot of Winchester and Floyd (1977a) was used in order to classify the primary igneous rock type and degree of differentiation (Fig. 3.8). The amphibolite, the metadiorite and the breccia cluster tightly in the andesite field, whereas the felsic dykes, being more evolved, as expected cluster in the rhyolite-rhyodacite field.

#### *Fractionation trendline*

In contrast to tholeiitic rocks, calc-alkaline rocks contain very few incompatible elements. Even the HFSE become compatible with magmatic differentiation in calc-alkaline rocks, and may not produce reliable magmatic trends (Liaghat and MacLean, 1995). When compatible, they generally cannot be used as immobile

**Figure 3.8** A  $\log (\text{Nb}/\text{Y})$  vs.  $\log (\text{Zr}/\text{TiO}_2)$  plot showing the compositions of the various igneous rock-types of the Troilus deposit. This diagram classifies the mafic rocks as andesite and the felsic dykes as dacite to rhyolite. Diagram after Winchester and Floyd (1977a).



elements to calculate mass changes. However, the two major elements Al and Ti, which also are immobile during alteration, exhibit almost linear compatibility during differentiation of calc-alkaline magmas, and may thus be used to track fractionation (Gibson and al. 1983, Campbell and al. 1984, MacLean and Kranidiotis 1987, MacLean, 1988, MacLean, 1990). We therefore used this pair of elements to monitor fractionation and to calculate mass changes in the Troilus rocks ("multiple precursor method" explained below).

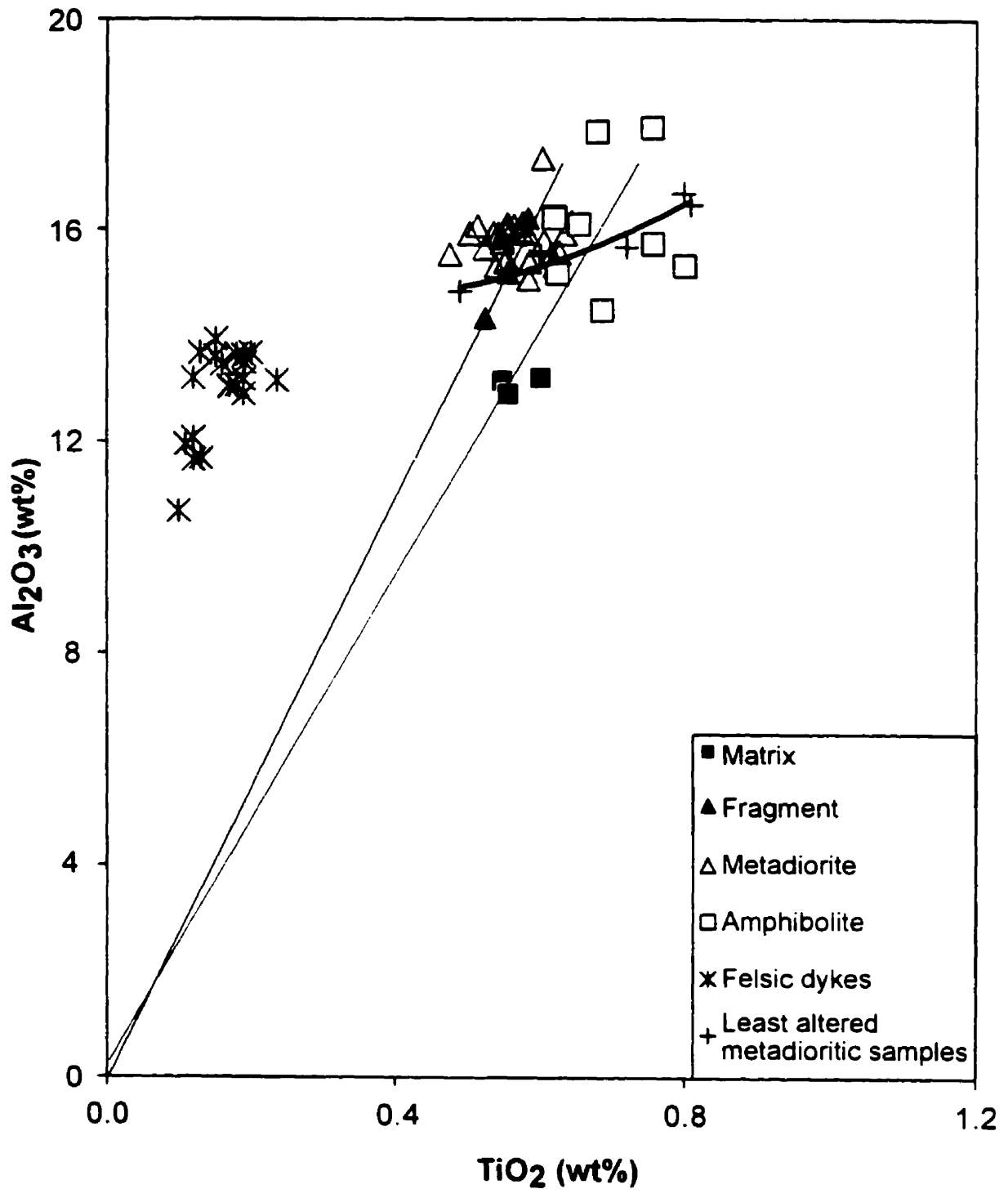
The equation of the fractionation line was determined from the five metadioritic samples considered to be the least altered, based on petrographic evidence (Fig. 3.9). The samples below the fractionation line are interpreted to have suffered a mass gain (dilution of the immobile elements) and the samples above, a mass loss (concentration of the immobile elements).

#### *Precursors of the breccia*

In order to gain insight into the origin of the breccia, matrix and fragment were mechanically separated from samples of a breccia collected outside the main ore zone, and were independently analyzed. If rocks have undergone varying degrees of mass change during alteration, immobile element pair data (like Ti and Al) spread along an alteration line, which passes through the origin (Fig.3.9). The intersection of this alteration line and the fractionation line discussed above yields the composition of the precursor of the altered rock.

As shown in figure 3.9, the matrix and the fragments have different compositions. The fragments scatter around the fractionation line while the matrix

**Figure 3.9** The composition of variably altered host rock samples of the Troilus deposit as a function of  $\text{TiO}_2$  and  $\text{Al}_2\text{O}_3$ . Lines passing through the origin represent the alteration lines. The bold curve represents the differentiation trendline based on the least altered samples. The point of intersection of an alteration line with a differentiation line represents the Ti and Al concentration of the precursor for a variably altered suite of samples.

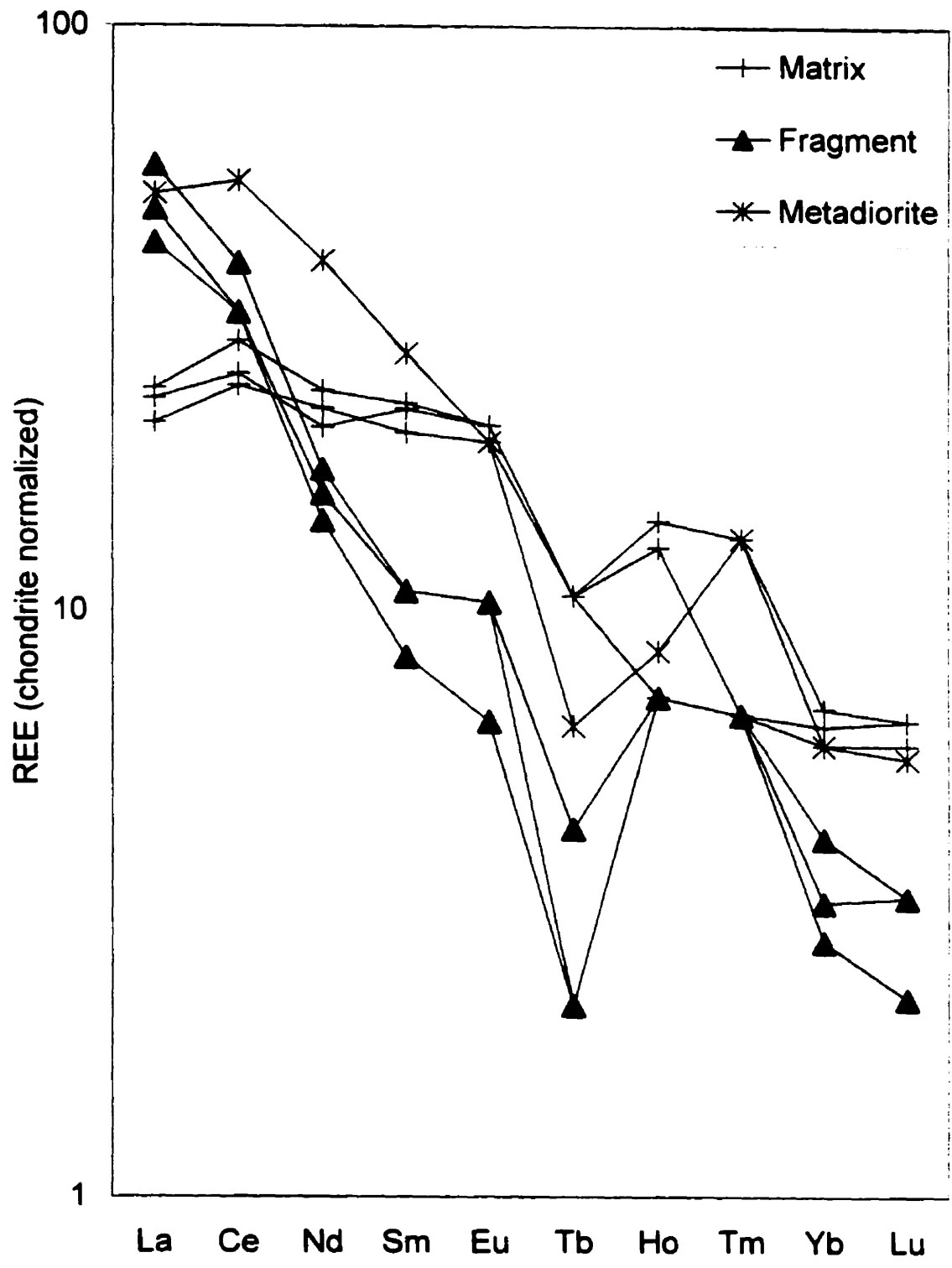


samples lie well below it, indicating that they suffered a higher degree of alteration. Moreover, alteration lines drawn from the origin through samples of the fragments and the matrix, crosscut the fractionation trendline at different points, suggesting that fragments and matrix have different precursors. The precursor of the fragments shows a lower Ti and Al content than the matrix, and plots with samples of metadiorite, while the precursor of the matrix plots with the amphibolite. The fragment and the metadiorite represent a slightly more evolved magma composition than the matrix and the amphibolite. This interpretation is confirmed by the REE profiles (Fig. 3.10); fragments and metadiorite have similar profiles, which differ from that of the matrix.

### **Petrography of the altered rocks**

There were two main stages of alteration associated with mineralization at Troilus: an earlier diffuse alteration now represented by abundant biotite (Stage 1) related to disseminated gold-copper-silver mineralization, and a sericitic alteration (Stage 2), which clearly overprints the biotitic alteration. This latter alteration is concentrated in high strain zones and is locally associated with high gold grades. In addition, there was a late stage of epidote-biotite alteration that locally accompanied minor remobilization of sulfides (Stage 3).

**Figure 3.10 Chondrite-normalized rare earth element profiles for the samples of fragment and matrix from the breccia and a least altered sample of metadiorite. The chondrite values used in normalizing REE are from Nakamura (1974).**



### *Stage 1 : Biotitic Alteration*

The nature of stage 1 alteration varies with lithology. Within the main ore zone, the amphibolite and the matrix to the breccia are altered to biotitic schists. The amphibolite consists of fine-grained, well-oriented biotite flakes (20 to 40 %), actinolitic hornblende and epidote (10 to 30 %), fine-grained quartz and feldspar (< 40 %), locally some garnet ( $\pm 5$  %) and some larger albite porphyroblasts ( $\pm 5$  %), which contain inclusions of quartz and fine biotite. Biotitization of the breccia is largely restricted to the matrix (from 30 to 60 % biotite), which also contains actinolitic hornblende (from 10 to 20 %), epidote (from 10 to 20 %), garnet ( $\pm 5$  %) and minor quartz. The fragments are composed of feldspar phenocrysts (40 %), ragged hornblende and epidote, with minor biotite in a fine-grained groundmass of quartz and feldspar. The matrix of the breccia and the amphibolite in the ore zone are strongly foliated, and although the fragments are neither foliated nor altered, they are highly deformed within the ore zone. The biotite-rich zones typically contain finely disseminated pyrite, chalcopyrite and/or pyrrhotite, as previously described under "Mineralization".

Biotitic alteration is also encountered in the metadiorite, which is locally cut by narrow 1 to 20 cm wide shears in which the rock becomes fine-grained and well foliated, and is mainly composed of quartz, biotite and plagioclase phenocrysts. These zones also contain disseminated sulfides and locally reach ore grade

The early phase of alteration also affected the felsic dykes, near contacts with the mafic rocks, where the dykes are fine-grained and comprise 2-3 mm thick alternating light and darker gray layers. The layering is determined by the nature of

the mica, some layers being biotite-rich and others muscovite-rich (due to the more felsic composition of the dykes). In both cases, the micas have a preferred orientation parallel to the compositional layering. Quartz forms 50-70% of the rock, and large sericitized plagioclase crystals are also present. Away from contacts with the mafic rocks, this early phase of alteration is characterized by a paragenesis of quartz (70%) and fine-grained muscovite (15%) with rare disseminated pyrite grains. Small, sericitized plagioclase grains may be present in the groundmass, and are more common where the rock contains a higher proportion of muscovite.

The intensity of the foliation of these altered rocks increases with their content of biotite, suggesting that alteration occurred prior to or at the same time as foliation development. The fact that peak metamorphic garnet is restricted to biotitic zones, in stable textural equilibrium with both fine biotite and amphibole, and with planar inclusion trails continuous with the external foliation, indicates that potassic alteration occurred prior to the peak of metamorphism. The biotite may represent primary hydrothermal biotite, or may be the metamorphic equivalent of the primary alteration assemblage (e.g. chlorite-sericite).

#### *Stage 2: Sericitic alteration*

Locally within the amphibolite, breccia and felsic dykes, there are zones of intense deformation slightly oblique to the main foliation, which have been strongly sericitized over widths up to several tens of centimeters. These zones are generally within a strongly silicified envelope several meters in width.

In the mafic rocks, sericitic alteration is represented by fine-grained and well-foliated quartz-muscovite schists, which commonly contain minor epidote and titanite, and several percent of disseminated euhedral pyrite, chalcopyrite and/or interstitial pyrrhotite. Muscovite may be restricted to the spaced cleavage where it has good preferred orientation, or it may replace the fine-grained biotite in zones which finger along the early foliation and late brittle structures. The spaced cleavage crosscuts the early foliation at a low angle and contains deformed garnet crystals, suggesting that sericitic alteration postdated the peak of metamorphism.

The intensity of sericitic alteration in sheared felsic dykes was evaluated quantitatively by point counting 500 grains per thin section across a high strain zone, and determining the proportion of minerals in each sample. From the least altered sample at the edge of a dyke to the core of the high strain zone, there is a 15% net increase in the sericite content and a corresponding loss of biotite. The most altered samples are composed essentially of a groundmass of equigranular quartz (60%) and well-oriented sericite crystals (40%) with traces of pyrite and chalcopyrite. Some perthitic feldspar phenocrysts and some garnet porphyroblasts may be present. The garnet crystals are elongate and skeletal, and contain inclusions of calcite. These rocks show a 2-3mm spaced cleavage at a low angle to the main foliation, marked by coarser muscovite flakes, tourmaline and chains of pyrite and/or pyrrhotite. Samples bordering the most intensively deformed parts of high-strain zones contain the highest proportion of quartz (66%) and sulfides (1.4%) in the felsic dykes.

### *Stage 3: Epidote-biotite alteration*

Cross-cutting sericitic alteration are patches of coarser epidote and biotite, which commonly also contain albite and granular garnet masses, along with some quartz, calcite and coarse-grained sulfides (mainly pyrite and pyrrhotite). This late alteration event seems to be associated with discordant veins and veinlets (millimeter thick) containing the assemblage quartz-biotite-calcite-epidote-amphibole-garnet-titanite-pyrite. No economic mineralization is associated with this alteration.

## **Alteration geochemistry**

### *Analytical method*

Most major elements (K, Na, Ca, Si, Fe, Mg, Mn) and many trace elements (Rb, Sr, Cs, Ba, etc.) are mobile during hydrothermal alteration associated with the formation of ore deposits (MacLean and Barrett, 1993). The calculation of mass changes for these elements yields quantitative information on hydrothermal alteration and fluid-rock interaction (Barrett, 1994). The mass additions represent net amounts of individual components that were brought into the altered rock from an external source via the hydrothermal fluids, while the mass losses are those of the components leached.

Mass changes within altered rocks from a variably differentiated magmatic suite may be calculated using the multiple precursor method (MacLean, 1990). In this method, the intersection of alteration and fractionation lines derived from an

immobile element pair yields the composition of the precursor of the altered magmatic unit. Based on the geochemical analysis of 50 samples from the Troilus deposit, Titanium appears to be the most immobile incompatible element for the mafic suite in this study, aluminum being slightly less immobile and the other commonly immobile elements (like Zr, Y and the REE) becoming variably compatible during crystallization of calc-alkaline magmas. Titanium was therefore chosen as the reference for the enrichment factor calculation. The trace elements having no simple polynomial relationships with the titanium, no reference line can be constructed to monitor the fractionation of trace elements, their mass change cannot be determined by the multiple precursor method.

#### *Mass changes for mafic rocks, Stage 1 alteration*

Relative mass changes (i.e. mass variation of an element in relation to the mass changes of the other major elements) and absolute mass changes (i.e. mass variation of an element in relation to the composition of the element itself) are presented in Figures 3.11 and 3.12, respectively. The altered samples of breccia were collected in the ore zone, where the proportion of the matrix represents about three to four times the proportion of fragments. Despite their heterogeneity, these samples still serve to indicate overall mass changes during alteration.

The amphibolite experienced an overall net mass loss of 1.88%, while the breccia suffered a net mass addition of 0.72%. However, amphibolite and breccia underwent essentially the same chemical changes, except for silica, the content of which is high in the fragments of the breccia. Potassium was added in the largest

**Figure 3.11 Histogram showing the average relative mass changes for each major mobile element in the different mafic units.**

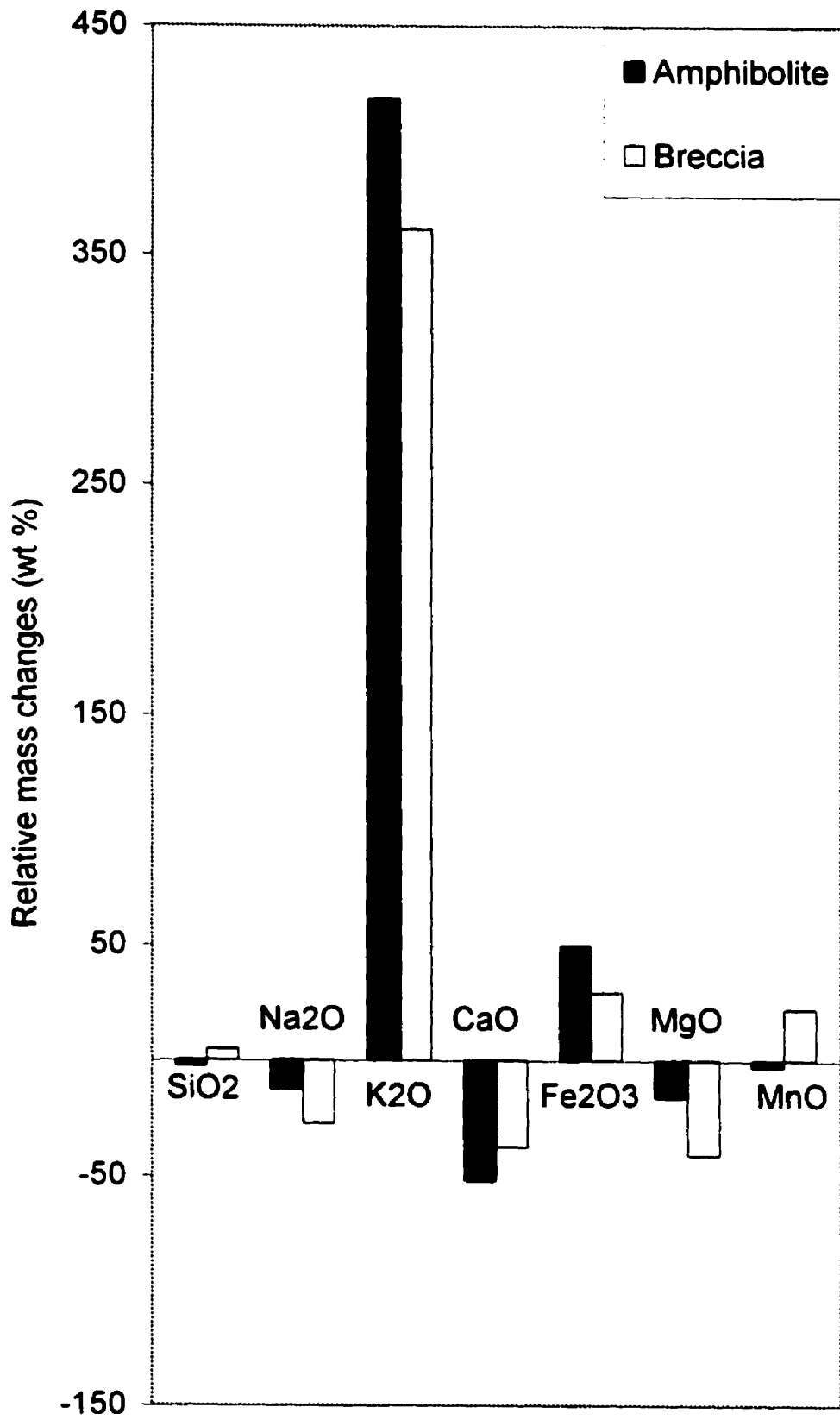
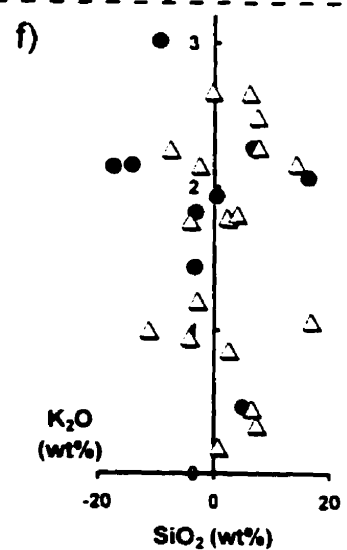
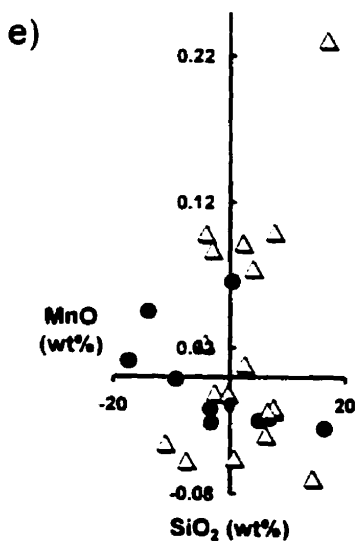
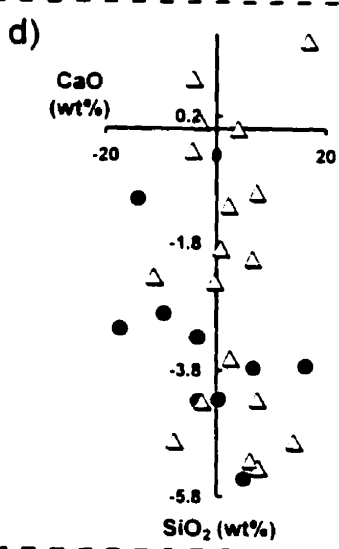
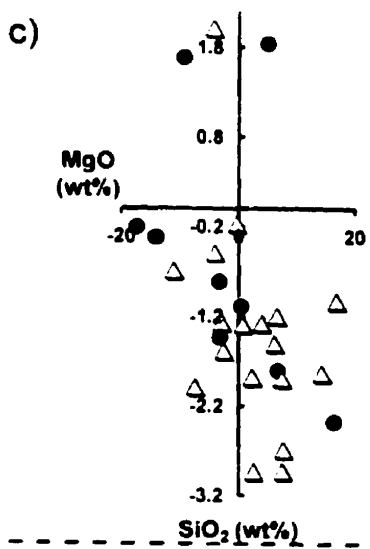
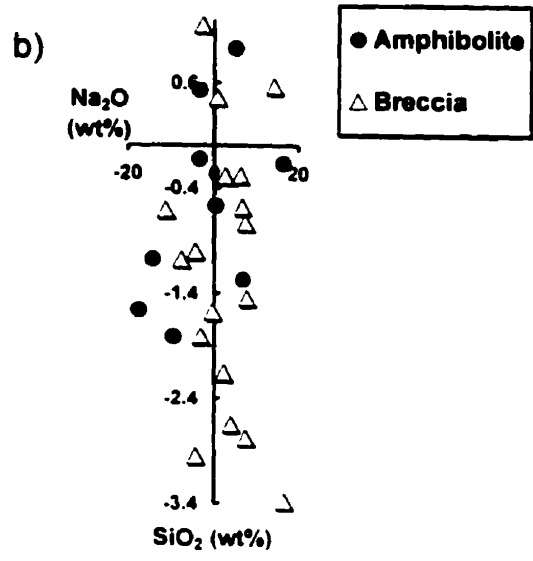
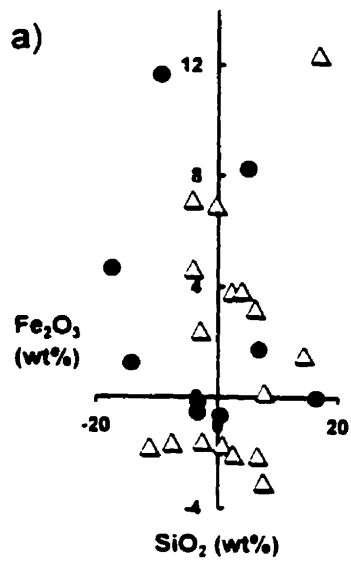


**Figure 3.12** Diagrams showing the absolute mass changes of mobile major elements versus the absolute mass changes of silica in the mafic rocks.



proportion relative to the other elements (relative mass additions of 418% and 361% in the amphibolite and the breccia, respectively).

Iron was added in the second highest proportion (50% and 30% relative mass additions in the amphibolite and the breccia, respectively), the addition being twice as much in the amphibolite as in the breccia. Except for two samples, magnesium was depleted in the amphibolite and the breccia. Mass changes in manganese were small, with no consistent trends. The silica mass changes were also small (Fig. 3.11). Sodium is depleted in the mafic rocks, except for three samples of breccia to which were added up to 20% of sodium. The amphibolite lost 50% of its calcium. In the breccia, the average mass loss in calcium was 35%, although a few samples apparently gained calcium, probably because of a higher proportion of fragments in these samples.

*Mass changes in felsic dykes, Stage 1 alteration.*

The mass changes in the felsic dykes are presented in Figures 3.13 and 3.14. The samples of the felsic dykes cluster on the  $\text{Al}_2\text{O}_3$  vs  $\text{TiO}_2$  graph, therefore mass changes were calculated relative to a single precursor. Sample #511 was chosen from the footwall dyke to represent the precursor, because of its low grade in gold and copper, and its low intensity of sulfidation, sericitization and silicification compared to the other samples. All samples from the hanging-wall dyke have suffered either stage 1 or stage 2 alteration, and no fresh samples were available.

**Figure 3.13** Histogram showing the average relative mass changes for each major mobile element in the felsic dykes.

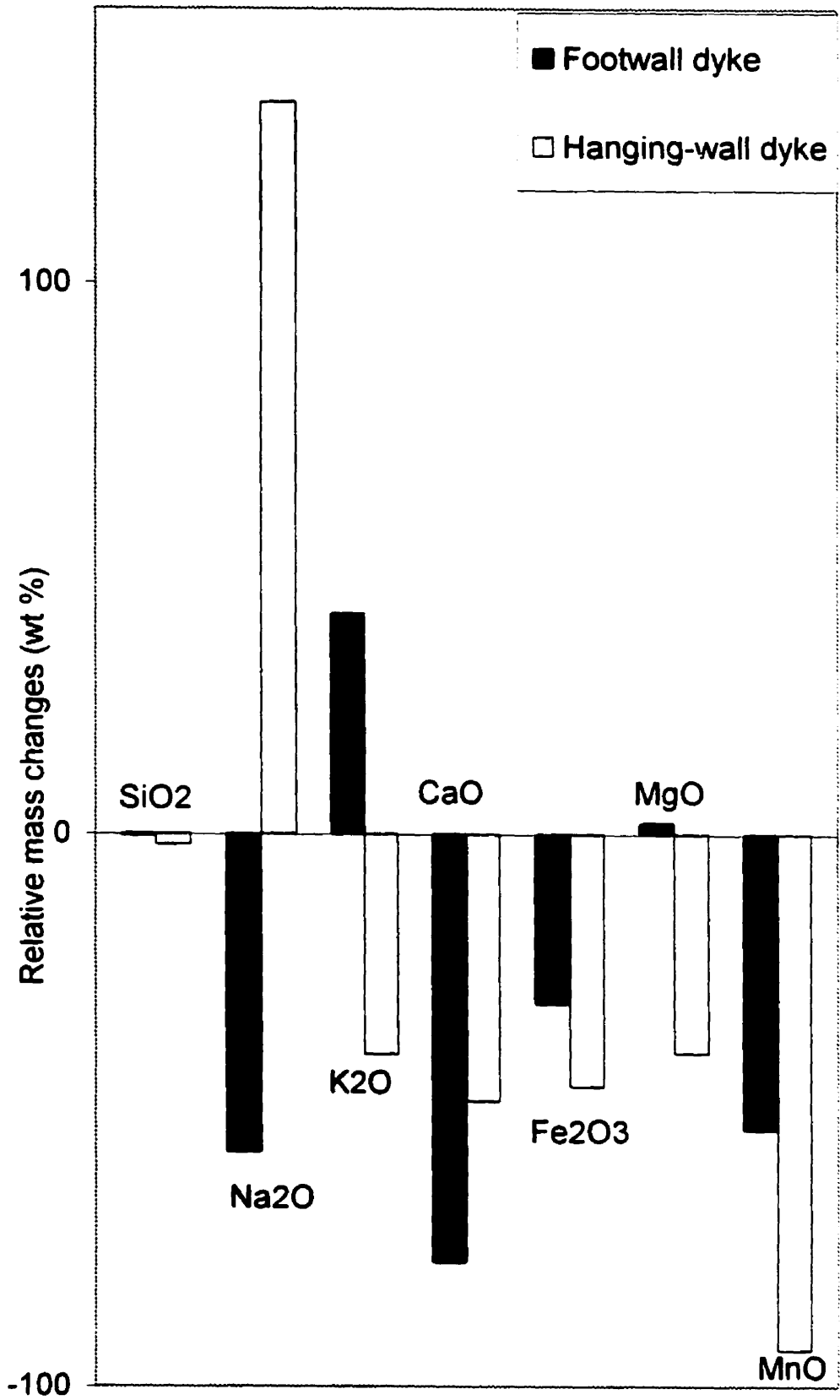


**Figure 3.14** Diagrams showing the absolute mass changes of mobile major elements versus the absolute mass changes of silica in the felsic dykes.



Aluminum was used as the reference for the calculations because of its immobility and its high concentration (low margin of error).

The samples analyzed for this study come from two dykes located in the 87 zone. The "footwall dyke" suite comprises nine samples from a large dyke to the east of the ore zone (structural footwall), and the "hanging-wall dyke" suite four samples from the dyke to the north-west of the ore zone (structural hanging wall). The hanging-wall and footwall dykes experienced a net mass loss of ~2%. Results from the footwall dyke indicate the same mass changes as for the mafic rocks. Potassium changed by +40% and sodium by -60%. Calcium, iron and manganese were leached, while magnesium and silica were essentially unchanged (Fig. 3.13). However, in the hanging-wall dyke, potassium and magnesium were depleted by 40% and 30%, and sodium enriched by 130%. Calcium, iron and manganese were leached and silica showed no significant change (Fig. 3.13). The difference in the mass changes for the two dykes may be due to their initial composition being slightly different (note that a sample from the footwall dyke was used to represent the precursor of both dykes). This emphasizes the importance of identifying the correct precursor rock when using this procedure.

Among the trace elements, strontium is depleted in the footwall dyke and enriched in the hanging-wall dyke, while rubidium is enriched in the footwall dyke and depleted in the hanging-wall dyke. Cerium, lanthanum and lithium are more depleted in the hanging-wall dyke than in the footwall dyke. The other trace elements do not show consistent trends.

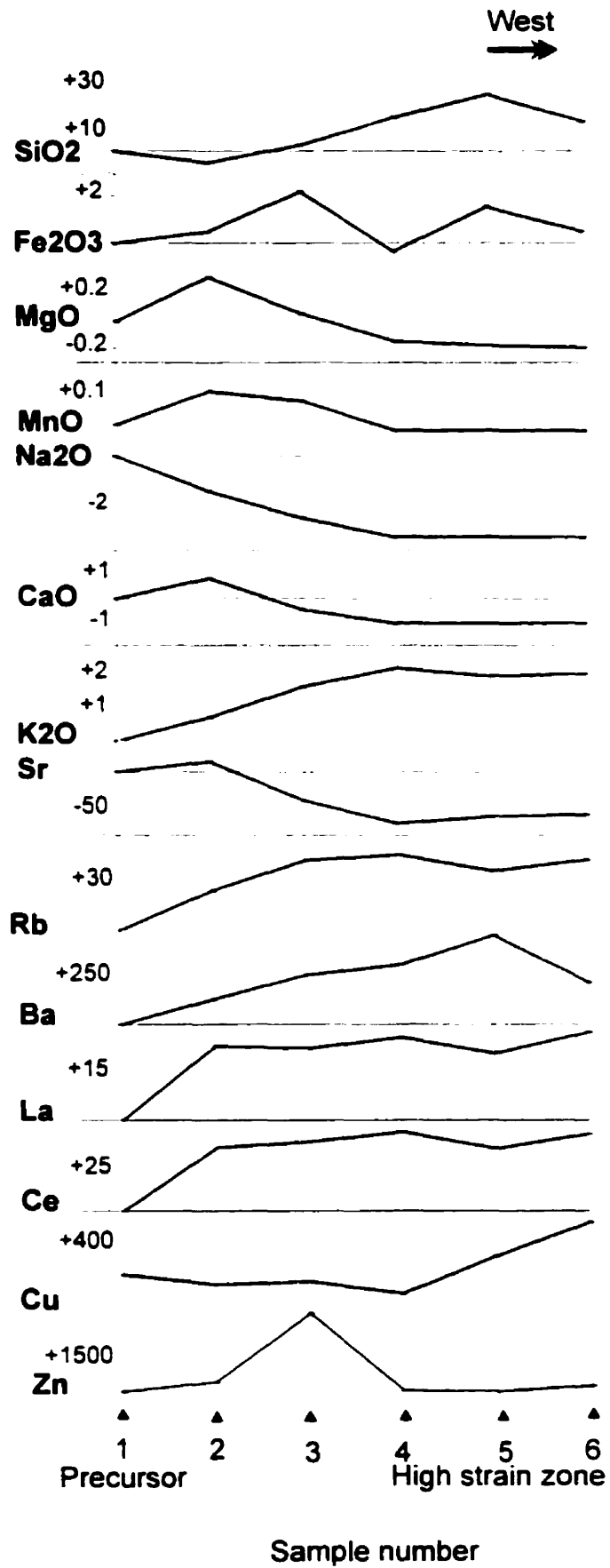
### *Mass changes, Stage 2 alteration*

Mass changes accompanying sericitic alteration were deduced from a suite of samples taken across a sericitized high strain zone in a felsic dyke. Seven samples were collected from the footwall dyke to the north-east of the 87 zone. The distances between adjacent samples were from 50 to 80 cm.

The sample farthest from the high strain zone was used to represent the precursor in mass change calculations. It is aphanitic, gray, homogeneous, contains only traces of sulfides, has a low concentration of sulfur and zinc, and an average concentration in copper compared to the other samples. Because of its well-established immobility,  $\text{Al}_2\text{O}_3$  was chosen to calculate the enrichment factor.

The results of the calculations of the absolute mass changes show that the samples situated within the shear zones have undergone large additions of silica and potassium, and depletions of sodium, calcium, magnesium, and manganese (Fig. 3.15). The addition of up to 30% silica to the shear zone is manifested as silicification of the felsic dykes, while the magnesium loss reflects the replacement of biotite by muscovite during the sericitization of the rock. Iron was added in some of the samples adjacent to the highly sericitized zone as pyrite, which also replaces biotite. Rubidium and barium behave similarly and follow the trend of potassium, increasing at a constant ratio, owing to their exclusive incorporation into sericite within the shear zones. Calcium and strontium behave similarly and are depleted within the shear zone. These results are not surprising given the affinity among K, Ba and Rb, and between Ca and Sr, two groups of elements having similar radius

**Figure 3.15** Diagrams showing absolute mass changes of the mobile elements across a high strain zone in a felsic dyke. The degree of deformation increases from the left to the right. The precursor used to monitor the mass changes is on the left of the graphs.



Sample number

and charge. Cerium and lanthanum were added to all the samples, relative to the precursor.

According to mine assay plans, the sericitic zone within the felsic dyke corresponds to a high-grade gold zone, containing 2.29 g/t gold. Similar zones elsewhere are also associated with high grades of gold, though copper grade tends to be erratic.

## Discussion

### *Previous interpretation of the Troilus deposit*

The only article that has been published on the Troilus deposit to date is that of Fraser (1993) who classified it as of porphyry-type, based on similarities to the Phanerozoic sub-volcanic-type class of porphyry deposits. Specifically he noted that the Troilus deposit is characterized by an association of disseminated and stringer styles of sulfide mineralization with zoned potassic and propylitic alteration assemblages, and is localized in a zone with multiple stages of felsic dykes and a mineralized *in situ* hydrothermal breccia, features that are typical of porphyry-type deposits. In addition to these characteristics, Boily (1998) interpreted the sericitization as typical of the phyllic alteration found in porphyry-type deposits.

Magnan (1993) came to a quite different conclusion in a MSc thesis on the petrography and geochemistry of the Troilus deposit. Based mainly on samples from a cross-section of the 87 zone, he concluded that the alteration, nature of the

mineralization, and the location of the deposit in a deformation corridor are more consistent with the deep-level mesothermal lode-gold model of Robert (1990).

The new exposure provided by the open pit and the data that have been collected during this study have permitted more extensive and detailed characterization of the alteration, deformation and mineralization and shed new light on the timing of the different hydrothermal events, the origin of the breccia and the role of the felsic dykes.

#### *Alteration and mineralization phases*

In view of the general acceptance of the porphyry model for the genesis of the Troilus deposit (Fraser, 1993; Boily, 1998) and the fact that Troilus is frequently cited in the literature as an example of an Archaean porphyry (e.g. Kirkham and Sinclair, 1995; Sillitoe, 2000), it is pertinent to compare the alteration at Troilus with that typically developed in porphyry systems.

Four principal alteration types may be developed in and around gold-rich porphyry copper deposits: potassium-silicate, propylitic, phyllic and argillic alteration (Sillitoe, 1993). In the generalized model of Lowell and Guilbert (1970), these alteration types are zonally distributed in and around the mineralized intrusion. They form shells with a core of potassic (K-feldspar) alteration grading outward through phyllic (sericite-pyrite), argillic and propylitic (chlorite-epidote) zones into unaltered country rock (Lowell and Guilbert, 1970). However, just as commonly, potassic alteration is dominated by biotite rather than orthoclase, the sericitic and argillic alteration are weakly developed or absent and the propylitic alteration lies peripheral to and replaces minerals of the potassic zone (Hollister, 1978). This is particularly

the case where the porphyry is of dioritic composition. It should also be noted that phyllic alteration commonly overprints potassic alteration and argillic alteration is generally restricted to the upper sub-volcanic parts of gold-rich porphyry systems. The potassium-silicate alteration is the most widely described, and perhaps most commonly seen (Titley, 1993).

The bulk of the gold in gold-rich porphyry deposits is introduced together with copper during this phase of alteration. Consequently, gold and copper grades usually vary sympathetically (Sillitoe, 1993).

As noted above, one of the principal lines of evidence used by Fraser (1993) to classify Troilus as a porphyry deposit is the presence of a core of biotite-rich potassic alteration surrounded by propylitic alteration.

Evidence collected during the course of our study shows that the gold-copper mineralized rocks generally contain 30 to 60 % of biotite, whereas the unmineralized equivalents are composed mainly of actinolitic hornblende and epidote, and contain little or no biotite. This local concentration of biotite in gold-copper mineralized rocks, together with evidence for the addition of potassium and depletion of sodium in both the mafic rocks and the felsic dykes (Fig. 3.11 and 3.13), and the positive correlation between the mass of potassium added and the copper content provide strong support for the argument that copper mineralization (with some gold) was accompanied by the pre-peak metamorphic biotite-rich potassic alteration described earlier in this article. However, this argument alone is not sufficient to classify Troilus as a porphyry-type deposit since potassic alteration is associated with mineralization in many Archaean deposits (Hodgson, 1993; Sillitoe, 1993).

In addition to the potassic alteration, another argument used by Fraser (1993) to support the porphyry model is the presence of a peripheral propylitic zone characterized by the assemblage albite-epidote-calcite. However, this alteration, which is best developed in the hanging wall, is expressed as randomly oriented grains of epidote, calcite and biotite and is seen only on late cleavage surfaces, indicating that it post-dated metamorphism. Therefore, it cannot be interpreted to represent porphyry-related propylitic alteration, i.e., it was not synchronous with the potassic alteration as required by the porphyry model (Sillitoe, 1993, Tittley, 1993). Instead the propylitic alteration of Fraser (1993) simply represents the latest hydrothermal event to have affected the Troilus deposit, postdating all mineralization and deformation.

The sericitic alteration described earlier in this study, was mentioned by Fraser (1993) but its significance was not discussed by him. However, Magnan (1993) and Boily (1998) interpreted the sericitization to represent the phyllic alteration usually encountered in porphyry-type deposits. Sericitization is restricted to high-strain zones and is characterized by a white to gray quartz-sericite assemblage representing partial to complete destruction of rock texture in the most deformed zones. It was accompanied by significant increases in potassium and silica and strong depletions of the other elements (Fig. 3.15). However, sericitization postdates peak metamorphism and regional deformation of the host rocks and developed significantly later than any hydrothermal activity that could have been associated with the crystallization and cooling of the magma forming the host rocks. Therefore, this alteration event cannot represent the phyllic alteration associated

with porphyry-style deposits. On the other hand, sericitization was of major importance in the history of the deposit. Mine assay data show that this alteration is associated with the highest gold grades, which locally reach over 100 g/t.

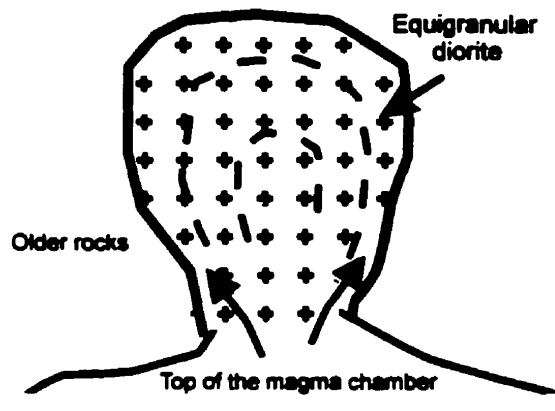
The two ore-related alteration events show major differences of: 1) timing (early, pre-peak metamorphic biotitization as opposed to a late, post-peak metamorphic sericitization), 2) types of mineralization (gold and copper in the early event and only gold in the late event), 3) and style of mineralization (the early phase is mainly disseminated, while the late phase is restricted to veins). These differences, particularly in timing, indicate that the two mineralizing events cannot represent two stages in the evolution of a single hydrothermal system. The Troilus deposit is therefore the result of two superimposed unrelated mineralization events, one of which introduced copper and gold and the other only gold. This discovery explains why no correlation was found between gold and copper, and why the gold grade of the Troilus deposit (1.08 g/t with a reserve of 51 Mt) is much higher than typical gold-rich porphyry deposits (according to data compiled by Sillitoe in 1993, only 2 of 27 deposits have a gold grade superior to 0.8 g/t and reserves lower than 100 Mt).

#### *Significance of the breccia*

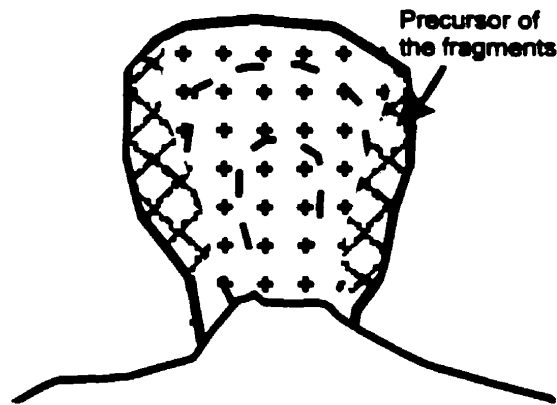
A common characteristic of porphyry-type deposits is the presence of an *in situ* hydrothermal breccia that carries higher copper and gold grades than surrounding stockwork and disseminated zones (Sillitoe, 1993). Fraser (1993) interpreted the breccia of the Troilus deposit to be of hydrothermal origin, and used

its presence as an important piece of evidence in favor of the porphyry model. According to this interpretation, the Troilus breccia formed by hydrofracturing of more competent rocks, creating a permeable zone through which hydrothermal fluids circulated and altered the rock, leaving remnants of less altered rock between anastomosing altered fracture zones. If this were the case, immobile element ratios in both fragment and matrix would have been the same despite their different degrees of alteration. However, the fragments and matrix have different immobile element ratios (Fig. 3.9), indicating that they have different magmatic precursors. The matrix of the breccia has a mineralogy and chemical signature similar to that of the amphibolite, while the fragments of the breccia are mineralogically and chemically comparable to the metadiorite. Moreover, the very similar chemical signatures of the metadiorite, the amphibolite and the breccia (Fig. 3.6 and Fig. 3.8) combined with the fact that their Ti-Al ratios are linearly related, conceivably representing a fractionation trendline, suggest that these different units have formed from the same primary magma. These geochemical features are consistent with an explanation in which the rocks form different parts of a single calc-alkaline pluton, which was intruded in several pulses at different stages of fractionation. The generation of the metadioritic pluton and the breccia is shown schematically in Figure 3.16. In this scheme, a first pulse of the magma with the composition of the metadiorite is intruded, cools and is fractured due to contraction or regional deformation. A second, more primitive pulse of magma, is intruded around the borders of the metadioritic pluton and within fractured metadiorite to form the geometry of the breccia and amphibolite around it.

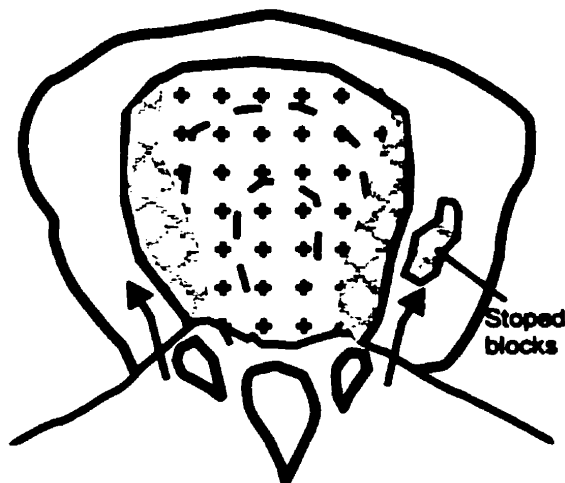
**Figure 3.16** Stages in the formation of the breccia. a. Stage 1: intrusion of a metadioritic pluton. b. Stage 2: Fracturing of the outer parts of the pluton due to contraction on cooling. c. Stage 3: intrusion of a second, more mafic, pulse of magma around the pluton and within its fractured outer parts.



**Stage 1: Intrusion of a calc-alkaline dioritic magma**



**Stage 2: Partial fracturing of the pluton due to cooling-induced contraction**



**Stage 3: Intrusion of a second pulse of magma around the pluton (precursor of amphibolite) and within the fractures of the diorite (precursor of the matrix of the breccia).**

The Troilus breccia, rather than being of hydrothermal origin and the main host rock of the deposit, is therefore a magmatic breccia formed by two separate magmatic components. This interpretation is of major importance since it eliminates one of the main arguments in favor of Troilus being a porphyry-type deposit, namely the presence of hydrothermal breccia. Moreover, if the above hypothesis is correct, the Troilus deposit is not hosted by volcanic rocks as previously thought (Fraser, 1993; Magnan, 1993) but by a calc-alkaline intrusive suite.

#### *The role of the felsic dykes*

Another important element of the porphyry model for the Troilus deposit (Fraser, 1993, Magnan, 1993, Boily 1998) is the presence of felsic dykes, which were believed to be contemporaneous with breccia development and mineralization. As seen previously on the Zr versus Y graph (Fig. 3.6), the felsic dykes plot in the calc-alkaline to transitional fields but the concentrations of Y and Zr differ significantly from those of the mafic rocks, as the dykes are more differentiated. Therefore the felsic dykes could be more evolved members of the same calc-alkaline suite as the metadiorite and amphibolite; they lie on the same fractionation line (Fig. 3.9). The gold-copper mineralization was believed by Fraser (1993) and Boily (1995) to be associated spatially, temporally and genetically with the felsic dykes. However, as seen from the petrography and mass change studies (Fig. 3.15), the felsic dykes were strongly affected by the late sericitization, but were poorly affected by the early potassic alteration and only near the contacts with the mafic rocks. Moreover, compilation of metal assays and descriptive logs of drill cores show

that copper in the main mineralized zone lies between two large felsic dykes, the “hanging-wall dyke” and the “footwall dyke” but not in them, whereas high gold values are also encountered in the felsic dykes and beyond them (Goodman, 2000). Therefore, the dykes cannot have been the source of the early gold-copper mineralization as previously believed, nor could they have acted as heat engines for hydrothermal activity. Rather they appear to have acted as barriers for the fluids, constraining the gold-copper mineralization to the mafic rocks between the hanging wall dyke and the footwall dyke. The spatial relationship between the mineralization and the felsic intrusions is most plausibly explained as being structurally controlled as is commonly the case in mesothermal deposits (Hodgson, 1993).

#### *Comparison with other lode gold deposits*

In the preceding paragraphs, we have shown that Troilus has been classified incorrectly as an example of an Archaean porphyry deposit. Instead many of its features are most consistent with Troilus being an Archaean lode deposit.

Most Archaean gold deposits belong to a coherent genetic group of structurally controlled lode-deposits. Although the majority of Archaean lode deposits represent the so-called “mesothermal” class, which is typically hosted in greenschist-facies rocks, a significant proportion of lode gold deposits occurs in amphibolite- to granulite-facies rocks (Groves, 1993). The mineralization may be found in any rock type, and ranges in form from veins and veinlet systems, to disseminated replacement zones (Hodgson, 1993). While the ore always shows clear spatial and genetic associations with contemporaneous structures, the accompanying alteration

assemblages vary in mineralogy with the metamorphic grade of the enclosing rocks. Under greenschist facies metamorphism, the dominant alteration assemblage is ankerite/dolomite-white mica-chlorite-biotite. However, at low to mid-amphibolite grade, amphibole-biotite-plagioclase assemblages are dominant, and the rocks are characteristically enriched in potassium and sulfur (Groves, 1993).

The potassium enrichment and the fact that the ore is restricted in a corridor structurally controlled by two felsic dykes favor the lode gold model for the first stage of mineralization of Troilus. The biotitic alteration, resulting from the potassium addition, is characteristic of lode gold deposits at the amphibolite facies (Groves 1993). For example, the Kolar deposit, India, is an Archaean lode gold deposit controlled by two major shear zones that predated the peak metamorphism, which reached the middle to the upper amphibolite facies (Hamilton and Hodgson, 1986). In the ore zone of this deposit, the first noticeable change in the amphibolite, as the gold veins are approached, is the appearance of biotite at the expense of amphibole. However, the first stage of mineralization at Troilus differs from other Archaean gold deposits in two important ways: 1) the gold was accompanied by significant copper and silver, whereas most Archaean gold deposits contain dominantly gold and only traces of other metals (Hodgson, 1993), and 2) the mineralization is disseminated with idiomorphic pyrite or occurs in millimeter wide sulfide veinlets, while Archaean gold deposits typically take the form of quartz lodes, which have a clear spatial and genetic association with structures like faults or shear zones.

With respect to the metal budget of the first stage of mineralization at Troilus, it should be noted that some Archaean lode gold deposits host significant proportions of base metals (Colvine et al., 1988). For example the Archaean Westonia gold deposit, located in the central Yilgarn craton, Western Australia, is characterized by a metal association of Au-Ag-W-Cu-Pb-Mo. The mineralization, localized in a series of quartz-rich veins within a broad shear zone and synchronous with peak, to slightly post-peak metamorphism (amphibolite facies), the alteration assemblages (mainly composed of quartz-feldspar-biotite), and the chemical changes accompanying alteration (addition of K, Rb and S, and loss of Na, Ca, Mg, and Sr) classify Westonia as an Archaean hypozonal lode gold deposits (Cassidy et al., 1998; Haggeman and Cassidy, 2000). The Boddington deposit, which was previously considered as an example of an Archaean porphyry deposit on the basis of its Au-Cu-Mo assemblage (Roth et al., 1990), has recently been interpreted as a mesothermal lode gold deposit of post-peak metamorphic age (Allibone et al., 1998). These examples are not the only ones: it has been shown that Ag and Cu abundances increase with a rise in temperature and pressure, i.e., the crustal depth of emplacement (Haggeman and Cassidy, 2000).

Finally, as noted above, the first stage of mineralization at Troilus differs from that of most Archaean gold deposits, in the dissemination of the gold, rather than its concentration in quartz veins, in many of the latter deposits (Colvine et al., 1988). For example, in the Archaean Wiluna gold deposit, Yilgarn craton, Western Australia, the bulk of the gold is disseminated in wall rocks and breccias that border a strike-slip fault system (Hagemann and Cassidy, 2000). Therefore, although the

style of stage 1 mineralization at Troilus is unusual for an Archaean lode gold deposit, it is not unprecedented.

The second, post-peak metamorphic mineralization, is more typical of lode gold deposits, being characterized by: 1) addition of large amounts of potassium and leaching of sodium, 2) mineralization restricted to high strain zones, 3) and gold in quartz-sulfide veinlets parallel to the spaced cleavage associated with the sericitization. The most unusual feature of the second stage of mineralization of Troilus compared to the major well-studied Archaean lode deposits, is the nature of the alteration, which consists exclusively of sericite and quartz. By contrast, most Canadian lode gold deposits showing sericitization, tend also to exhibit carbonate-dominated alteration, e.g. Sigma mine, Abitibi (Robert and Brown, 1984), Cameron Lake, Ontario (Melling et al., 1986), the Hollinger and McIntyre deposit, Ontario (Burrows and Spooner, 1986). However, unlike Troilus, all these deposits are hosted in greenschist grade rocks. If the compilation is restricted to lode gold deposits within amphibolite grade rocks, the alteration assemblage is typically carbonate-poor, and potassium- and sulfide-rich (Colvine et al., 1988).

The Troilus deposit is the result of two superimposed hydrothermal systems, one pre-metamorphic, and one post-metamorphic. Although most of the lode gold deposits appear to have formed under syn-peak-metamorphic conditions, several pre- and post-peak metamorphism lode gold deposits are known from the Yilgarn Block, Australia and the Abitibi greenstone belt, Canada (Groves, 1993). The superimposition of mineralization at Troilus was the result of two pulses of

hydrothermal fluid flow, at different times in the regional metamorphic history of the deposit, but both apparently at relatively deep crustal levels.

## **Conclusions**

The objective of this study was to characterize the alteration and mineralization of the Troilus deposit in order to place some constraints on genetic modeling. The main conclusions of the study are:

- The host rock is a calc-alkaline metadioritic pluton intruded as, at least, two pulses of magma at slightly different stages of differentiation.
- An initial stage of hydrothermal activity was pre-peak metamorphic and introduced disseminated gold-copper-silver mineralization in association with biotitic alteration. This type of mineralization is restricted to the mafic rocks and is bounded by two felsic dykes.
- Felsic dykes, which are also calc-alkaline and were also intruded prior to peak metamorphism, could be more evolved members of the same calc-alkaline suite. They acted as barriers to the ore fluids that introduced the early copper-gold mineralization for the early hydrothermal event.
- The second mineralizing event was post-metamorphic and produced veinlet-style gold mineralization accompanied by sericitic alteration in high-strain zones within felsic dykes, amphibolite and breccia.
- The evidence that led earlier researchers to propose a porphyry-type model for the Troilus deposit has been re-evaluated: 1) the felsic dykes were not the

source of the fluids for the mineralization; 2) propylitic alteration did not accompany potassic alteration, 3) sericitic alteration is post-peak metamorphic and is not linked to magmatism, 4) the Troilus breccia, rather than being of hydrothermal origin and the main host rock of the deposit, is a magmatic breccia. Troilus is therefore not an example of an Archaean porphyry copper-gold deposit.

- Despite some unusual features, probably due to the depth of formation, the two hydrothermal events that formed Troilus are similar to the deeper counterpart of the classic orogenic gold deposits occurring at the greenschist facies, as described in the continuum model of Groves (1993).

## **CHAPTER IV: CONCLUSIONS**

The main conclusions of the study are:

- 1) The Troilus domain, which hosts the Troilus gold-copper deposit, consists of a coarse- to medium-grained metadiorite, a finer-grained amphibolite, a rock with a brecciated texture and felsic dykes, which crosscut the metadioritic pluton, the amphibolite and the breccia.
- 2) The chemical signature of the immobile elements, Ti, Al, Y and Zr, and the REE show that all these units are calc-alkaline, whereas the mafic lavas and dykes that surround the deposit are of tholeiitic affinity.
- 3) Metadiorite, amphibolite and breccia are part of the same calc-alkaline suite. Metadiorite and fragments of the breccia were formed during a first pulse of magma. A second, more primitive pulse of magma intruded around the borders of the metadioritic pluton and within fractured metadiorite to form the geometry of the breccia and amphibolite around it.
- 4) The chemical signature of immobile and compatible elements (Ti and Al) shows that the felsic dykes may represent more evolved rocks from the same magma source.
- 5) An initial stage of hydrothermal activity was pre-peak metamorphic and introduced gold-copper-silver mineralization. This type of mineralization comprises disseminated pyrite and sulfide stringers parallel to the foliation. It is restricted to the biotitized amphibolite and matrix to the breccia, and is bounded by two major felsic dykes.

- 6) Early mineralization was accompanied by an enrichment in potassium and iron and a loss in sodium and calcium, now represented by fine-grained biotite in the mafic units and fine-grained muscovite in the felsic dykes.
- 7) The second mineralizing event, which was post-metamorphic, is restricted to high-strain zones and produced quartz veinlet-style gold mineralization, which crosscuts the main foliation. This stage of mineralization was accompanied by sericitization within felsic dykes, amphibolite and breccia. In these high strain zones, the rocks suffered a significant addition of potassium and a loss in sodium and calcium. Silica was enriched in the wall rocks of the deformed zones, forming a silicified envelope several meters thick, in which the quartz-sulfide veins are more abundant.
- 8) The evidence that led earlier researchers to propose a porphyry-type model includes nature and distribution of alteration (potassic-phyllitic-propylitic), the presence of felsic dykes as a potential source for the fluid, and a hydrothermal breccia as the most mineralized rock unit. The results of this study show that:
- Propylitic alteration did not accompany potassic alteration.
  - Sericitic alteration was post-peak metamorphic and not linked to magmatism.
  - The felsic dykes predated mineralization and were therefore not the source of the ore fluids.
  - The Troilus breccia, rather than being of hydrothermal origin and the main host rock of the deposit, is a magmatic breccia.

Troilus is therefore not an example of an Archaean porphyry copper-gold deposit.

- 9) The first stage of mineralization has features common to lode gold deposits, namely the widely spread biotitic alteration, the potassium addition, and the fact that the mineralization is confined to a corridor. However, the lack of quartz veins and the presence of significant copper are unusual, although they have been previously documented in some lode gold deposits.
- 10) The second stage of mineralization is more characteristic of lode gold deposits, having gold-rich quartz veinlets, potassium addition and sodium depletion, and structurally-controlled mineralization. However, although muscovite is often encountered as an alteration mineral in Archaean lode gold deposits, it is usually accompanied of carbonate, except, significantly, in deposits hosted by amphibolite facies rocks.
- 11) Despite these features, the two stages of mineralization at Troilus are similar to the more deeply seated examples of classic orogenic gold deposits described in the continuum model of Groves (1993).

## REFERENCES

Allibone, A.H., Windh, J., Etheridge, M.A., Burton, D., Anderson, G., Edwards, P.W., Miller, A., Graves, C., Fanning, C.M., and Wysoczanski, R., 1998, Timing relationships and structural controls on the location of Au-Cu mineralization at the Boddington gold mine, Western Australia, *Economic Geology*, v. 93, p. 245-273.

Barrett, T.J., 1993, Mass changes in hydrothermal alteration zones associated with VMS deposits of the Noranda area, *Exploration and Mining Geology*, v. 3, No. 2, p. 131-160.

Barrett, T.J., and MacLean, W.H., 1991, Chemical, mass and oxygen isotope changes during extreme hydrothermal alteration of an Archaean rhyolite, Noranda, Quebec, *Economic Geology*, v. 86, pp. 406-414.

Boily, B., 1995, The lac Troilus deposit, *in* Pilote, P., Dion, c., and Morin, R., *Metallogeny and geologic evolution of the chibougamau mining area-from porphyry cu-Au-Mo to mesothermal lode gold deposits*, Geological Survey of Canada, open file 3143, p. 123-130.

Boily, B., 1998, Géologie et métallogénie du district minier de Chapais-Chibougamau: ICM and MRNQ DV 98-03.

Bourne, J.H., 1973, Mesgouez Lek area, Mistassini and New Quebec territories, MRNQ DP-110.

Burrows, D.R., and Spooner, E.T.C., 1986, The McIntyre Cu-Au deposit, Timmins, Ontario, Canada, *in* MacDonald A.J., ed., Proceedings of Gold '86, an International Symposium on the Geology of Gold, p. 23-39.

Campbell, I.H., Lesher, C.M., Coad, P., Franklin, J.M., Gorton, M.P., and Thurston, P. C., 1984, Rare-earth element mobility in alteration pipes below massive Cu-Zn sulfide deposits, *Chemical Geology*, v. 2, p. 181-202.

Carson, D. J.T., 1990, Mineralogy and predictive metallurgy of the Frotet Lake Deposit, Unpublished technical report.

Cassidy, K.F., Groves, D. I., and McNaughton, N.J., 1998, Late-Archean granitoid-hosted lode gold deposits, Yilgarn craton, Western Australia: Deposit characteristics, crustal architecture and implications for ore genesis, *Ore Geology Reviews*, v. 13, p. 1013-1016.

Colvine, A.C., 1989, An empirical model for the formation of Archean gold deposits: products of final cratonization of the Superior Province, Canada ECONOMIC GEOLOGY, Monograph 6, p.37-53.

Colvine, A.C., Fyon, J.A., Heather, K.B., Marmont, S., Smith, P.M., and Troop, D.G., 1988, Archean lode gold deposits in Ontario, Ontario Geological Survey, Miscellaneous Paper 39, 136 p.

David, J., 1999, Projet Grand-Nord: Géochronologie: nouvelles données et mise en perspective, *in* Lalonde, J.P., ed., Explorer au Québec: Le défi de la connaissance, programmes et résumés, 1999, DV 99-03.

Dion, C., Pilote, P., David, J., Cater, D., 1998, Géologie et âge de la minéralisation Au-Cu à la mine Troilus, ceinture de Frotet-Evans, Québec, GAC abstracts, v. 46.

Fraser, R.J., 1993, The Lac Troilus gold-copper deposit, northwestern Quebec: a possible Archaean porphyry system, *Economic Geology*, v. 88, p. 1685-1699.

Gibson, H.L., Watkinson, D.H., Watkins, J.J., Labrie, M., and Dorion, G., 1993, Volcanological reconstruction of the Corbet breccia pile, and Cu-Zn massive sulfide deposit, Noranda, Quebec, *Explor. Min. J.*, v. 2, p. 1-16.

Goodman, S., 2000, The Troilus research project: Activity report of March 2000, internal report.

Gosselin, C., 1993, Géologie de l'extrémité NE de la bande volcano-sédimentaire de Frotet-Troilus, MERQ MB 93-03.

Gosselin, C., 1994, Géologie de l'extrémité nord-est de la bande volcano-sédimentaire de Frotet-Troilus, MRNQ MB 94-06.

Gosselin, C., 1996, Synthèse géologique de la région de Frotet-Troilus, MRNQ ET 96-02.

Groves, D.I., 1993, The crustal continuum model for late-Archaeon lode-gold deposits of the Yilgarn Block, Western Australia, Mineralium Deposita, v. 28, p.366-374.

Groves, D. I., Barley, M. E. , Barnicoat, A. C., Cassidy, K. F., Fare, R. J. , Hagemann, S. G., Ho, S. E., Hronsky, J. M. A., Mikucki, E. J., Mueller, A. G., McNaughton, N. J., perring, C. S., Ridley, J. R., and Vearncombe, J. R., 1992, Sub-greenschist to granulite-hosted Archaean lode-gold deposits of the Yilgarn Craton: a depositional continuum from deep-sourced hydrothermal fluids in crustal-scale plumbing systems, Geology Department (Key Centre) and

University Extension. The University of Western Australia Publication 22, p. 325-337.

Gunter, W., 1973, Bueil Lake area, Abitibi and Mistassini territories, MRNQ DP-137.

Gunter, W., 1977, Région du lac Bueil: MRNQ RG-189.

Hagemann, S.G., and Cassidy, K.F., 2000, Archean orogenic lode gold deposits, *in*, Hagemann, S.G, and Brown, P.E., eds., Gold in 2000, Society of Economic Geologists reviews, v. 13, p.9-68.

Hamilton, J.V., and Hodgson, C.J., 1986, Mineralization and structure of the Kolar Gold Field, India, *in* MacDonald, A.J., ed., Proceedings of Gold '86, An International Symposium of the Geology of Gold, p.270-283.

Hocq, M., 1974, Région du lac Miskittenau, Territoire de Mistassini, MRNQ DP-276.

Hocq, M., 1978, Région du lac Miskittenau, MRNQ DPV-550.

Hocq, M., 1994, Géologie du Québec, p.1-19.

Hodgson, C.J., 1993, Mesothermal lode-gold deposits, *in* Kirkham, R.V., Sinclair, W.D., Thorpe, R.I., and Duke, J.M., eds., Mineral deposit modeling: Geological Association of Canada, Special paper 40, p. 635-678.

Hollister, V.F., 1978, Geology of the porphyry copper deposits of the Western Hemisphere, New York Society of Mining Engineers AIME, 219 p.

Kirkham, R.V., and Sinclair, W.D., 1995, Porphyry copper, gold, molybdenum, tungsten, tin, silver, Minister of Natural Resources Canada, ed., Geology of Canadian mineral deposit types, chapter 19, p.421-446.

Kuhns, R.J., 1986, Alteration styles and trace element dispersion associated with the Golden Giant deposit, Hemlo, Ontario, Canada. In: MacDonald A.J.(ed.) Proceeding of gold '86, p. 340-354.

Leshner, C.M., Goodwin, A.M., Campbell, I.H. and Gorton, M.P., 1986, Trace-element geochemistry of ore-associated and barren, felsic metavolcanic rocks in the Superior Province, Canada. Canadian Journal of Earth Sciences, v. 23, p. 222-237.

Liaghat, S., and MacLean, H., 1995, Lithogeochemistry of altered rocks at the New Inco VMS deposit, Noranda, Quebec, Journal of Geochemical Exploration, v. 52, p. 333-350.

Lowell, J.D., and Guilbert, J.M., 1970, Lateral and vertical alteration-mineralization zoning in porphyry ore deposits, *Economic Geology*, v. 65, p. 373-408.

MacLean, W.H., 1988, Rare earth element mobility at constant inter-REE ratios in the alteration zone at the Phelps Dodge massive sulfide deposit, Matagami, Quebec, *Mineralium Deposita*, v. 23, p. 231-238

MacLean, W.H., 1990, Mass change calculations in altered rock series, *Mineralium Deposita*, v. 25, p. 44-49.

MacLean, W.H., and Barrett, T.J., 1993, Lithogeochemical techniques using immobile elements, *Journal of Geochemical Exploration*, v. 48, p.109-133.

MacLean, W.H., and Hoy, L.D., 1991, Geochemistry of hydrothermally altered rocks at the Horne mine, Noranda, Quebec, *Economic Geology*, v.86, p. 506-528.

MacLean, W.H., and Kranidiotis, P., 1987, Immobile elements as monitors of mass transfer in hydrothermal alteration: Phelps Dodge massive sulfide deposit, Matagami, Quebec, *Economic Geology*, v. 82, p. 951-962.

Magnan, M., 1993, La Zone 87 du gisement d'or et de cuivre du lac Troilus: pétrographie et géochimie. MSc thesis, Université du Québec à Chicoutimi.

McMillan, W. J., and Panteleyev, A., 1980, Porphyry copper deposits, *in Ore deposit models*, ed. Roberts R. G. and Sheahan P.A. Geoscience Canada, p. 45-58.

Melling, D.R., Watkinson, D.H., Poulsen, K.H., Chorlton, L.B., and Hunter, A.D., 1986, The Cameron Lake gold deposit, northwestern Ontario: Geological setting, structure, and alteration, *in MacDonald A.J., ed., Proceedings of Gold '86, an International Symposium on the Geology of Gold*, p. 149-169.

Nakamura, N., 1974, Determination of REE, Ba, Fe, Mg, Na and K in carbonaceous and ordinary chondrites, *Geochemica et Cosmochemica Acta*, v. 38, p. 757-775.

Palmer, M., 1972, Geological report of Lac Mésière project, SDBJ/Selco Min. Corp. MERQ GM-34062.

Pearce, J.A. and Cann, J.R., 1973, Tectonic setting of basic volcanic rocks determined using trace element analysis, *Earth and Planetary Sciences Letters*, v. 19, p. 290-300.

Pilote, P., Dion, C., Joanisse, A., David, J., Machado, N., Kirkham, R.V., Robert, F., 1997, Géochronologie des minéralisations d'affiliation magmatique de l'Abitibi, secteurs Chibougamau et de Troilus-Frotet: implications géotectoniques, ed. Ministère des Ressources Naturelles, Québec, DV 97-03, p.47.

Richardson, S.V., Kesler, S.E., Essene, E.J., and Jones, L.M., 1986, Origin and geochemistry of the Chapada Cu-Au deposit, Goias, Brazil: a metamorphosed wall-rock porphyry copper deposit, *Economic Geology*, v. 81, p. 1884-1898.

Robert, F., 1990, An overview of gold deposits in the eastern Abitibi subprovince, *in* The northwestern Quebec polymetallic belt. Ed. Rive et al., Canadian Institute of Mining and Metallurgy, special volume 43, p. 93-105.

Robert, F., and Brown, A.C, 1984, Progressive alteration with gold-quartz-tourmaline veins at the Sigma mine, Abitibi greenstone belt, Quebec, *Economic Geology*, v. 81, p. 587-592.

Roth E., Bennett J.M., and Symons P.M., 1990, Boddington and Black Flag: anomalous archaean gold deposits, *in* Gold deposits of the Archaean Yilgarn block, Western Australia: nature, genesis and exploration guides, Chapter 1.

Shriver, N.A., and MacLean, W.H., 1993, Mass, volume and chemical changes in the alteration zone at the Norbec mine, Noranda, Quebec, *Mineralium Deposita*, v. 28, p.157-166.

Sillitoe R. H., 1993, Gold-rich porphyry copper deposits: geological model and exploration implications, in Kirkham R. V., Sinclair W. D., Thorpe R. I. and Duke J. M., Ed. *Mineral deposit modeling: Geological Association of Canada*, special paper 40, p. 465-478.

Sillitoe, R.H., 2000, Role of gold-rich porphyry deposit models in exploration, *in* Hagemann, S.G, and Brown, P.E., eds., *Gold in 2000*, Society of Economic Geologists reviews, v. 13, p. 315-345.

Simard, A., 1982, Demie sud du canton 1423, MERQ DP 82-02.

Simard, A., 1983, Lithostratigraphie préliminaire de la partie est de la bande volcano-sédimentaire archéenne Frotet-Evans, MERQ EWT 82-01, p.163-176.

Simard, A., 1985, Evolution du volcanisme archéen dans la région du lac Troilus, MERQ ET 83-18.

Simard, A., 1987, Stratigraphie et volcanisme dans la partie orientale de la bande volcano-sédimentaire archéenne Frotet-Evans, MERQ MB 87-17.

Sinclair W. D., 1982, Gold deposits of the Matachewan area, Ontario, *in* Hodder R.W., and Petruk W., Ed. *Geology of Canadian gold deposits: Canadian Institute of Mining and Metallurgy, special volume 24*, p. 83-93.

Symons, P.M., Anderson, G., Beard, T.J., Hamilton, L.M., Reynolds, G.D., Robinson, J.M., and Staley, R.W., 1988, The Boddington gold deposit, *in* Goode, A.D.T., and Bosma, L.I., compilers, *Bicentennial Gold 88, Melbourne symposium 1988: Geological Society of Australia, Abstracts, v. 22*, p. 56-61.

Titley, S.R., 1993, Characteristics of porphyry copper occurrence in the American southwest, *in* Kirkham R.V., Sinclair, W.D., Thorpe, R.I., and Duke, J.M., ed., *Mineral deposit modeling: Geological Association of Canada, Special Paper 40*, p. 433-464.

Watson, E.B., and Harrison, T.M., 1983, Zircon saturation revisited: temperature and composition effects in a variety of crustal magma types. *Earth and Planetary Sciences Letters*, v. 64, p. 295-304.

Whitford, D.J., McPherson, W.P.A., and Wallace, D.B., 1989, Geochemistry of the host rocks of the volcanogenic massive sulfide deposit at Que River, Tasmania, *Economic Geology*, v. 84, p. 1-21

Wilson, M., 1989, *Igneous petrogenesis: a global tectonic approach*, Chapman & Hall, chapter 2.

Winchester P.A. and Floyd P.A., 1977(a), *Geochemical discrimination of different magma series and their differentiation products using immobile elements*, *Chemical Geology*, v. 20, p. 325-343.

Winchester P.A. and Floyd P.A., 1977(b), *Identification and discrimination of altered and metamorphosed volcanic rocks using immobile elements*, *Chemical Geology*, v. 21, p. 291-306.

## **APPENDICES**

## **APPENDIX I**

### **Geochemical Host Rock Analysis**

The analyses were made for major and trace element compositions at the Centre de Recherche Minérale (CRM). All samples were analyzed by X-ray fluorescence (XRF) spectrometry techniques for the major elements as well as for Rb, Ga, Nb, Sr, Y and Zr. The concentrations of rare-earth elements and other trace elements were determined by instrumental neutron activation analysis (INAA).

The major element analyses have been calculated as a percentage.

For the trace elements, the detection limit is 300 ppm for Cu, Zn, Mo, and Pb, 100 ppm for Ni, 50 ppm for Ba, 2 ppm for Ce and La, 1 ppm for the other trace elements, and less than 0.5 ppm for the rare earth elements (0.1 ppm for Lu).

**APPENDIX I**  
**Geochemical Host Rock Analysis (%)**

<b>Amphibolite</b>	<b>Al<sub>2</sub>O<sub>3</sub></b>	<b>CaO</b>	<b>Cr<sub>2</sub>O<sub>3</sub></b>	<b>Fe<sub>2</sub>O<sub>3</sub></b>	<b>K<sub>2</sub>O</b>	<b>MgO</b>	<b>MnO</b>	<b>Na<sub>2</sub>O</b>	<b>P<sub>2</sub>O<sub>5</sub></b>	<b>SiO<sub>2</sub></b>	<b>TiO<sub>2</sub></b>
1998019804	14.49	3.68	0.50	5.31	2.28	1.56	0.05	3.59	0.19	67.67	0.68
1998019808	15.32	3.43	0.51	12.92	0.89	5.67	0.05	4.31	0.24	55.87	0.80
1998019858	15.18	3.40	0.04	16.89	3.40	4.77	0.07	2.58	0.07	52.98	0.62
1998019812	17.93	6.33	0.49	7.93	3.00	3.50	0.14	3.83	0.27	55.82	0.76
1998019809	15.74	4.15	0.49	7.47	2.66	2.32	0.06	2.77	0.22	63.36	0.76
1998019870	16.25	1.57	0.03	5.62	2.41	1.29	0.03	5.41	0.16	66.61	0.62
1998019873	16.23	2.64	0.03	5.20	2.00	1.95	0.04	4.71	0.16	66.43	0.62
1998019876	16.11	2.08	0.03	5.11	2.49	2.08	0.14	4.07	0.15	67.09	0.65
1998019880	17.86	3.02	0.02	11.81	3.02	2.81	0.08	3.51	0.22	56.98	0.68
<b>Breccia</b>	<b>Al<sub>2</sub>O<sub>3</sub></b>	<b>CaO</b>	<b>Cr<sub>2</sub>O<sub>3</sub></b>	<b>Fe<sub>2</sub>O<sub>3</sub></b>	<b>K<sub>2</sub>O</b>	<b>MgO</b>	<b>MnO</b>	<b>Na<sub>2</sub>O</b>	<b>P<sub>2</sub>O<sub>5</sub></b>	<b>SiO<sub>2</sub></b>	<b>TiO<sub>2</sub></b>
1998019814	15.66	1.67	0.52	5.91	2.73	0.95	0.18	2.87	0.15	68.69	0.69
1998019806	14.99	1.63	0.51	8.53	2.98	1.99	0.04	3.88	0.13	64.67	0.65
1998019823	16.18	1.47	0.01	4.06	2.75	1.03	0.05	6.08	0.15	67.61	0.61
1998019857	16.12	4.74	0.01	4.06	0.67	2.02	0.02	5.09	0.12	66.49	0.67
1998019868	15.07	4.86	0.02	2.38	0.77	0.89	0.04	3.73	0.13	71.52	0.59
1998019807	13.06	7.82	0.51	14.47	1.24	2.64	0.25	0.54	0.15	58.67	0.65
1998019871	14.54	5.23	0.03	12.00	1.32	4.49	0.08	3.36	0.14	58.25	0.56
1998019863	15.07	6.32	0.02	9.97	2.18	1.95	0.15	1.62	0.14	62.01	0.56
1998019860	16.20	2.59	0.05	2.75	3.06	0.56	0.06	1.66	0.16	72.22	0.69
1998019813	16.78	3.73	0.50	3.96	1.42	0.83	0.10	4.27	0.16	67.51	0.74
1998019802	15.36	5.63	0.50	9.33	2.20	1.71	0.17	2.13	0.13	62.16	0.67
1998019864	15.54	6.07	0.03	8.03	1.68	1.48	0.15	2.77	0.15	63.49	0.60
1998019824	15.06	3.80	0.01	3.32	0.88	1.56	0.04	3.88	0.11	70.75	0.58
1998019831	14.63	5.98	0.01	8.94	2.14	1.76	0.14	1.71	0.12	63.98	0.60
1998019833	17.99	1.28	0.01	4.54	3.17	1.03	0.01	4.02	0.15	67.09	0.71
1998019895	17.76	3.74	0.03	4.20	1.68	2.02	0.01	4.66	0.15	65.09	0.66
1998019872	14.08	1.67	0.01	6.53	2.36	1.49	0.01	4.44	0.14	68.67	0.60
1998019874	14.53	3.38	0.03	11.78	2.95	2.53	0.05	2.78	0.14	61.26	0.57
<b>Fragment only</b>	<b>Al<sub>2</sub>O<sub>3</sub></b>	<b>CaO</b>	<b>Cr<sub>2</sub>O<sub>3</sub></b>	<b>Fe<sub>2</sub>O<sub>3</sub></b>	<b>K<sub>2</sub>O</b>	<b>MgO</b>	<b>MnO</b>	<b>Na<sub>2</sub>O</b>	<b>P<sub>2</sub>O<sub>5</sub></b>	<b>SiO<sub>2</sub></b>	<b>TiO<sub>2</sub></b>
1999029251	16.26	4.33	0.02	4.07	0.48	0.71	0.02	5.76	0.13	67.64	0.58
1999029252	15.22	5.20	0.02	5.60	0.39	0.71	0.02	4.72	0.12	67.45	0.55
1999029253	14.37	4.65	0.02	5.14	0.45	0.91	0.02	4.73	0.12	69.05	0.52
<b>Matrix only</b>	<b>Al<sub>2</sub>O<sub>3</sub></b>	<b>CaO</b>	<b>Cr<sub>2</sub>O<sub>3</sub></b>	<b>Fe<sub>2</sub>O<sub>3</sub></b>	<b>K<sub>2</sub>O</b>	<b>MgO</b>	<b>MnO</b>	<b>Na<sub>2</sub>O</b>	<b>P<sub>2</sub>O<sub>5</sub></b>	<b>SiO<sub>2</sub></b>	<b>TiO<sub>2</sub></b>
1999029255	13.21	8.75	0.02	23.07	1.03	4.79	0.10	1.86	0.12	46.45	0.60
1999029256	13.16	9.29	0.02	23.88	0.80	5.07	0.11	2.07	0.12	44.93	0.55
1999029257	12.91	8.42	0.02	25.32	1.12	5.38	0.11	2.18	0.12	43.87	0.55
<b>Diorite</b>	<b>Al<sub>2</sub>O<sub>3</sub></b>	<b>CaO</b>	<b>Cr<sub>2</sub>O<sub>3</sub></b>	<b>Fe<sub>2</sub>O<sub>3</sub></b>	<b>K<sub>2</sub>O</b>	<b>MgO</b>	<b>MnO</b>	<b>Na<sub>2</sub>O</b>	<b>P<sub>2</sub>O<sub>5</sub></b>	<b>SiO<sub>2</sub></b>	<b>TiO<sub>2</sub></b>
1999029259	15.69	7.83	0.02	6.68	0.44	4.15	0.09	4.11	0.17	60.11	0.72
1999029260	16.70	8.42	0.02	5.26	0.45	4.18	0.09	4.24	0.15	59.70	0.80
1999029261	16.49	8.14	0.02	6.40	0.61	4.27	0.09	4.25	0.16	58.76	0.81
1999029265	15.53	4.70	0.01	5.16	1.33	2.55	0.06	4.34	0.14	65.58	0.60
1999029258	16.76	7.16	0.02	6.87	0.65	3.96	0.10	4.80	0.15	58.85	0.69
1999029262	14.85	5.39	0.01	1.68	0.42	1.64	0.03	4.89	0.12	70.48	0.49

**APPENDIX I (CONT'D)**  
**Geochemical Host Rock Analysis (%)**

<b>Felsic dykes</b>	<b>Al<sub>2</sub>O<sub>3</sub></b>	<b>CaO</b>	<b>Cr<sub>2</sub>O<sub>3</sub></b>	<b>Fe<sub>2</sub>O<sub>3</sub></b>	<b>K<sub>2</sub>O</b>	<b>MgO</b>	<b>MnO</b>	<b>Na<sub>2</sub>O</b>	<b>P<sub>2</sub>O<sub>5</sub></b>	<b>SiO<sub>2</sub></b>	<b>TiO<sub>2</sub></b>
1998019815	13.16	0.02	0.49	4.40	3.67	0.46	0.20	0.95	0.06	76.36	0.24
1998019817	13.49	0.49	0.01	1.72	3.83	0.47	0.06	1.19	0.02	78.53	0.19
1998019819	13.93	0.58	0.01	1.96	4.08	0.55	0.11	0.88	0.04	77.72	0.15
1998019820	13.62	0.52	0.01	1.69	3.83	0.45	0.13	0.67	0.04	78.88	0.15
1998019821	11.66	0.40	0.01	1.68	3.06	0.53	0.09	0.46	0.04	81.94	0.12
1998019822	11.69	0.39	0.01	1.69	3.08	0.52	0.09	0.50	0.04	81.84	0.13
1998019827	12.90	1.88	0.01	2.88	2.57	0.55	0.15	2.18	0.03	76.66	0.19
1998019834	13.18	1.41	0.01	1.44	1.86	0.58	0.05	3.96	0.02	77.29	0.19
1998019848	13.62	0.29	0.01	1.77	4.39	0.63	0.03	0.70	0.02	78.35	0.19
1998019849	13.03	0.84	0.01	1.43	1.70	0.14	0.01	5.26	0.02	77.39	0.17
1998019853	13.68	1.16	0.01	1.57	3.74	0.71	0.03	1.22	0.02	77.67	0.20
1998019877	11.95	0.02	0.01	2.50	3.51	0.07	0.01	0.16	0.03	81.61	0.11
1998019878	13.19	0.57	0.01	4.26	3.34	0.55	0.10	0.95	0.03	76.87	0.12
1998019879	13.67	1.05	0.01	2.23	1.75	0.46	0.03	3.60	0.04	77.02	0.13
1998019881	12.08	0.02	0.01	1.70	3.63	0.15	0.01	0.17	0.03	82.07	0.12
1998019882	10.70	0.02	0.01	3.09	3.10	0.09	0.01	0.17	0.03	82.68	0.10
1998019890	13.46	1.34	0.01	2.14	2.71	0.55	0.04	2.57	0.05	76.97	0.16
1998019851	13.05	0.86	0.01	1.87	1.57	0.28	0.01	5.33	0.02	76.83	0.17
1998019852	13.65	1.32	0.01	1.85	1.65	0.63	0.01	4.93	0.01	75.77	0.18
1998019847	13.06	0.97	0.01	1.26	1.41	0.32	0.01	5.23	0.02	77.54	0.18
1998019884	13.38	0.79	0.02	2.30	3.31	0.79	0.07	1.23	0.05	77.93	0.14
1998019885	13.99	1.97	0.01	2.81	2.59	1.15	0.14	2.19	0.04	74.96	0.14
<b>Pillow lavas</b>	<b>Al<sub>2</sub>O<sub>3</sub></b>	<b>CaO</b>	<b>Cr<sub>2</sub>O<sub>3</sub></b>	<b>Fe<sub>2</sub>O<sub>3</sub></b>	<b>K<sub>2</sub>O</b>	<b>MgO</b>	<b>MnO</b>	<b>Na<sub>2</sub>O</b>	<b>P<sub>2</sub>O<sub>5</sub></b>	<b>SiO<sub>2</sub></b>	<b>TiO<sub>2</sub></b>
1998019854	14.91	8.36	0.02	12.48	0.31	5.02	0.24	2.58	0.08	54.78	1.21
1998019856	15.00	9.36	0.02	12.24	0.35	4.69	0.27	2.64	0.08	54.17	1.18
1998019883	15.71	8.27	0.04	12.08	0.71	3.75	0.22	1.93	0.10	55.98	1.22
1998019861	15.29	8.97	0.04	13.98	0.49	3.33	0.26	2.38	0.14	53.37	1.74
1998019862	14.47	9.68	0.04	15.48	0.53	3.61	0.28	1.90	0.14	52.22	1.64
<b>Mafic dykes</b>	<b>Al<sub>2</sub>O<sub>3</sub></b>	<b>CaO</b>	<b>Cr<sub>2</sub>O<sub>3</sub></b>	<b>Fe<sub>2</sub>O<sub>3</sub></b>	<b>K<sub>2</sub>O</b>	<b>MgO</b>	<b>MnO</b>	<b>Na<sub>2</sub>O</b>	<b>P<sub>2</sub>O<sub>5</sub></b>	<b>SiO<sub>2</sub></b>	<b>TiO<sub>2</sub></b>
1998019803	15.55	3.53	0.59	11.51	2.08	2.99	0.08	4.24	0.15	58.45	0.84
1998019801	16.06	11.21	0.56	11.81	1.97	6.72	0.21	1.36	0.06	49.38	0.67

**APPENDIX I (CONT'D)**  
**Geochemical Host Rock Analysis (ppm)**

<b>Amphibolite</b>	<b>Ba</b>	<b>Ce</b>	<b>Co</b>	<b>Cu</b>	<b>Ga</b>	<b>La</b>	<b>Li</b>	<b>Mo</b>	<b>Nb</b>	<b>Ni</b>	<b>Pb</b>	<b>Rb</b>
1998019804	306	42	10	33	16	22	17	9	3	37	12	84
1998019808	76	54	40	15	19	27	18	5	5	115	16	39
1998019858	379	15	69	375	18	9	28	4	3	164	12	141
1998019812	894	72	23	34	18	40	28	4	4	16	12	84
1998019809	234	58	22	9	18	28	48	4	5	25	18	92
1998019870	387	12	16	942	19	6	26	4	3	35	12	80
1998019873	445	17	14	82	22	10	25	4	3	31	12	68
1998019876	423	13	13	45	21	8	24	4	3	33	12	75
1998019880	373	41	68	311	21	23	42	4	6	62	12	111

<b>Amphibolite (cont'd)</b>	<b>Sc</b>	<b>Sm</b>	<b>Sr</b>	<b>V</b>	<b>Y</b>	<b>Zn</b>	<b>Zr</b>
1998019804	10	4.00	238	81	11	40	126
1998019808	20	6.00	417	152	13	59	136
1998019858	21	4.00	270	122	16	54	106
1998019812	14	6.00	716	142	13	96	133
1998019809	11	6.00	240	94	17	52	163
1998019870	11	2.00	186	101	10	66	116
1998019873	16	2.00	188	103	14	132	116
1998019876	17	2.00	178	117	11	78	116
1998019880	19	2.00	268	121	13	186	120

<b>Breccia</b>	<b>Ba</b>	<b>Ce</b>	<b>Co</b>	<b>Cu</b>	<b>Ga</b>	<b>La</b>	<b>Li</b>	<b>Mo</b>	<b>Nb</b>	<b>Ni</b>	<b>Pb</b>	<b>Rb</b>
1998019814	382	16	14	700	19	7	19	4	3	27	35	162
1998019806	620	15	38	7000	20	9	35	4	3	84	12	131
1998019823	491	19	14	89	17	10	23	4	3	26	12	162
1998019857	108	21	14	143	19	11	11	4	3	42	12	131
1998019868	182	33	5	322	17	20	11	4	3	16	12	162
1998019807	143	7	47	117	19	6	30	4	3	119	12	131
1998019871	150	19	33	380	24	12	18	4	3	57	12	162
1998019863	320	17	15	107	18	9	36	4	3	53	12	131
1998019860	537	24	7	1	19	12	28	4	3	14	20	162
1998019813	373	22	9	71	19	10	32	4	3	20	12	131
1998019802	385	18	24	20	19	12	48	4	3	63	12	162
1998019864	323	17	17	100	19	10	49	4	3	51	12	131
1998019824	190	28	15	12	17	16	9	4	3	38	12	162
1998019831	334	24	19	53	18	14	36	4	3	58	16	131
1998019833	454	14	11	1000	23	5	18	4	3	35	12	162
1998019895	254	23	10	610	21	12	24	4	4	30	12	131
1998019872	436	15	23	2900	19	8	40	4	3	52	12	162
1998019874	609	24	34	2000	19	14	34	4	3	64	12	131

<b>Fragment only</b>												
1999029251	220	29	10	9	17	18	-	3	4	19	1	13
1999029252	50	22	12	290	16	14	-	1	4	22	1	8
1999029253	74	31	16	17	14	20	-	2	5	23	1	10

<b>Matrix only</b>												
1999029255	200	21	61	1300	27	8	-	1	5	120	9	27
1999029256	190	22	67	220	28	7	-	1	6	120	4	13
1999029257	200	23	64	120	29	8	-	1	4	140	2	30

**APPENDIX I (CONT'D)**  
**Geochemical Host Rock Analysis (ppm)**

<b>Breccia (cont'd)</b>	<b>Sc</b>	<b>Sm</b>	<b>Sr</b>	<b>V</b>	<b>Y</b>	<b>Zn</b>	<b>Zr</b>
1998019814	8	3.00	98	90	15	125	112
1998019806	21	2.00	187	115	13	57	109
1998019823	10	3.00	180	99	13	38	118
1998019857	14	5.00	374	124	8	34	124
1998019868	10	2.00	282	82	11	27	113
1998019807	55	3.00	151	111	15	161	106
1998019871	16	2.00	304	114	13	150	111
1998019863	15	2.00	168	115	10	102	109
1998019860	10	6.00	208	118	12	27	127
1998019813	12	5.00	263	108	10	19	118
1998019802	18	3.00	180	104	12	66	108
1998019864	16	2.00	223	105	11	45	113
1998019824	13	5.00	353	87	9	51	113
1998019831	18	8.00	161	117	14	99	110
1998019833	12	2.00	119	142	13	40	119
1998019895	12	4.00	331	118	18	36	128
1998019872	13	2.00	157	103	10	89	108
1998019874	12	2.00	245	86	9	62	108

**Fragment only**

1999029251	7.2	1.80	379	-	6	4	119
1999029252	7	2.40	443	-	9	4	114
1999029253	7.2	2.40	361	-	9	9	107

**Matrix only**

1999029255	29	4.70	156	-	18	52	101
1999029256	25	4.30	126	-	18	47	101
1999029257	21	4.90	139	-	18	66	99

<b>Diorite</b>	<b>Ba</b>	<b>Ce</b>	<b>Co</b>	<b>Cu</b>	<b>Ga</b>	<b>La</b>	<b>Li</b>	<b>Mo</b>	<b>Nb</b>	<b>Ni</b>	<b>Pb</b>	<b>Rb</b>
1999029259	150	45	21	15	18	18	-	1	5	64	1	6
1999029260	110	40	19	13	18	17	-	1	6	50	1	7
1999029261	120	48	20	12	19	18	-	1	5	60	1	12
1999029265	310	59	21	19	18	31	-	3	7	23	1	39
1999029258	230	33	24	41	19	17	-	1	5	56	1	13
1999029262	130	56	9	8	16	24	-	1	9	7	1	9

<b>Diorite (cont'd)</b>	<b>Sc</b>	<b>Sm</b>	<b>Sr</b>	<b>V</b>	<b>Y</b>	<b>Zn</b>	<b>Zr</b>
1999029259	19	4.90	473	-	16	65	106
1999029260	19	5.10	478	-	17	44	93
1999029261	20	6.30	470	-	18	52	86
1999029265	12	4.90	460	-	16	39	183
1999029258	18	3.70	489	-	14	67	93
1999029262	9.4	5.00	465	-	16	18	221

**APPENDIX I (CONT'D)**  
**Geochemical Host Rock Analysis (ppm)**

<b>Felsic dykes</b>	<b>Ba</b>	<b>Ce</b>	<b>Co</b>	<b>Cu</b>	<b>Ga</b>	<b>La</b>	<b>Li</b>	<b>Mo</b>	<b>Nb</b>	<b>Ni</b>	<b>Pb</b>	<b>Rb</b>
1998019815	355	78	3	200	15	41	45	4	8	2	66	114
1998019817	362	95	5	419	14	52	17	4	11	3	42	130
1998019819	287	81	13	2500	13	44	13	4	9	8	22	62
1998019820	425	103	7	492	16	55	18	4	10	8	86	126
1998019821	414	95	5	85	15	50	15	4	8	2	107	105
1998019822	393	80	8	837	14	43	13	4	8	2	15	86
1998019827	388	100	3	18	14	54	31	4	8	4	37	72
1998019834	423	91	4	73	16	48	10	4	9	4	223	39
1998019848	603	97	4	168	14	55	21	4	8	9	19	122
1998019849	803	55	4	223	15	26	7	4	8	4	13	28
1998019853	497	92	4	14	15	48	19	4	8	5	17	101
1998019877	401	84	7	963	13	46	5	4	8	1	12	84
1998019878	464	85	14	299	16	44	16	4	8	2	17	89
1998019879	220	50	9	398	17	23	11	4	8	2	12	48
1998019881	480	84	5	145	14	44	7	4	8	1	12	86
1998019882	564	69	13	517	12	36	8	4	8	1	12	70
1998019890	375	88	8	448	12	48	15	4	9	6	12	60
1998019851	554	66	3	339	13	34	6	4	9	9	17	32
1998019852	480	84	14	295	17	44	9	4	6	14	12	38
1998019847	434	68	3	249	14	35	7	4	9	4	15	31
1998019884	550	95	3	21	16	50	50	4	10	3	25	113
1998019885	366	88	8	284	15	48	23	4	11	3	15	76

<b>Felsic dykes (cont'd)</b>	<b>Sc</b>	<b>Sm</b>	<b>Sr</b>	<b>V</b>	<b>Y</b>	<b>Zn</b>	<b>Zr</b>
1998019815	3	6.00	28	2	20	1200	149
1998019817	4	12.00	67	4	29	41	177
1998019819	4	7.00	131	2	21	42	167
1998019820	5	10.00	70	3	32	86	187
1998019821	5	8.00	53	3	29	78	175
1998019822	3	7.00	60	2	26	251	155
1998019827	3	9.00	112	2	28	7000	142
1998019834	3	9.00	85	3	21	268	152
1998019848	3	10.00	51	4	18	117	147
1998019849	4	8.00	137	2	28	41	173
1998019853	3	9.00	67	2	24	88	158
1998019877	4	4.00	44	2	27	267	161
1998019878	4	4.00	68	2	28	3600	171
1998019879	3	2.00	116	2	28	61	177
1998019881	4	4.00	31	2	28	78	159
1998019882	4	2.00	37	2	21	33	145
1998019890	6	6.00	72	2	20	84	184
1998019851	4	9.00	137	2	25	30	175
1998019852	4	7.00	128	17	13	22	172
1998019847	4	8.00	136	2	18	35	176
1998019884	4	6.00	100	2	25	34	154
1998019885	4	5.00	137	2	29	514	184

**APPENDIX I (CONT'D)**  
**Geochemical Host Rock Analysis (ppm)**

<b>Pillow lavas</b>	<b>Ba</b>	<b>Ce</b>	<b>Co</b>	<b>Cu</b>	<b>Ga</b>	<b>La</b>	<b>Li</b>	<b>Mo</b>	<b>Nb</b>	<b>Ni</b>	<b>Pb</b>	<b>Rb</b>
1998019854	163	9	41	23	17	5	27	4	4	68	12	0.01
1998019856	201	16	42	38	19	7	27	4	4	70	12	0.01
1998019883	227	10	50	102	19	6	38	4	3	73	12	0.04
1998019861	247	12	60	101	23	5	37	4	5	115	12	0.29
1998019862	200	11	52	123	21	8	39	4	5	101	12	0.29

<b>Pillow lavas (cont'd)</b>	<b>Sc</b>	<b>Sm</b>	<b>Sr</b>	<b>V</b>	<b>Y</b>	<b>Zn</b>	<b>Zr</b>
1998019854	38	2.00	226	270	18	120	79
1998019856	39	2.00	245	272	19	116	78
1998019883	42	2.00	199	300	20	97	83
1998019861	38	2.00	194	354	31	133	99
1998019862	39	4.00	180	351	35	142	97

<b>Mafic dykes</b>	<b>Ba</b>	<b>Ce</b>	<b>Co</b>	<b>Cu</b>	<b>Ga</b>	<b>La</b>	<b>Li</b>	<b>Mo</b>	<b>Nb</b>	<b>Ni</b>	<b>Pb</b>	<b>Rb</b>
1998019803	524	62	30	1600	20	45	23	19	3	107	12	0.31
1998019801	311	5	50	25	17	4	26	4	3	111	12	0.09

<b>Mafic dykes (cont'd)</b>	<b>Sc</b>	<b>Sm</b>	<b>Sr</b>	<b>V</b>	<b>Y</b>	<b>Zn</b>	<b>Zr</b>
1998019803	20	11.00	205	152	18	140	83
1998019801	48	2.00	300	251	15	181	40

**APPENDIX I (CONT'D)**  
**Geochemical Host Rock Analysis (ppm)**

<b>Amphibolite</b>	<b>Y</b>	<b>La</b>	<b>Ce</b>	<b>Nd</b>	<b>Sm</b>	<b>Eu</b>	<b>Tb</b>	<b>Ho</b>	<b>Tm</b>	<b>Yb</b>	<b>Lu</b>
1998019804	11.00	20.00	40.00	19.00	3.70	0.90	0.30	0.50	0.20	1.00	0.14
1998019812	13.00	40.00	83.00	37.00	6.20	1.70	0.40	0.60	0.50	1.20	0.19
<b>Breccia</b>	<b>Y</b>	<b>La</b>	<b>Ce</b>	<b>Nd</b>	<b>Sm</b>	<b>Eu</b>	<b>Tb</b>	<b>Ho</b>	<b>Tm</b>	<b>Yb</b>	<b>Lu</b>
1998019811	14.00	11.00	22.00	12.00	2.60	0.70	0.30	0.50	0.20	1.20	0.18
<b>Fragment only</b>											
1999029251	6.00	16.00	28.00	9.00	1.70	0.50	0.10	0.50	0.20	0.60	0.07
1999029252	9.00	14.00	28.00	10.00	2.20	0.80	0.20	0.50	0.20	0.70	0.11
1999029253	9.00	19.00	34.00	11.00	2.20	0.80	0.10	0.50	0.20	0.90	0.11
<b>Matrix only</b>											
1999029255	18.00	7.60	22.00	13.00	4.50	1.60	0.50	0.50	0.20	1.30	0.20
1999029256	18.00	6.90	21.00	14.00	4.10	1.50	0.50	1.00	0.40	1.50	0.22
1999029257	18.00	7.90	25.00	15.00	4.60	1.60	0.50	0.90	0.20	1.40	0.22
<b>Diorite</b>	<b>Y</b>	<b>La</b>	<b>Ce</b>	<b>Nd</b>	<b>Sm</b>	<b>Eu</b>	<b>Tb</b>	<b>Ho</b>	<b>Tm</b>	<b>Yb</b>	<b>Lu</b>
1999029259	16.00	18.00	50.00	25.00	5.20	1.40	0.40	0.80	0.20	1.30	0.21
1999029260	17.00	17.00	47.00	25.00	5.60	1.50	0.30	0.60	0.40	1.30	0.19
1999029261	18.00	18.00	57.00	29.00	6.60	1.60	0.30	1.60	0.50	1.50	0.16
1999029265	16.00	34.00	70.00	29.00	5.70	1.20	0.10	0.70	0.20	1.40	0.20
1999029258	14.00	18.00	41.00	20.00	4.10	1.20	0.40	1.00	0.20	1.50	0.18
1999029262	16.00	23.00	64.00	24.00	5.10	1.20	0.10	0.90	0.20	1.90	0.17
<b>Felsic dykes</b>	<b>Y</b>	<b>La</b>	<b>Ce</b>	<b>Nd</b>	<b>Sm</b>	<b>Eu</b>	<b>Tb</b>	<b>Ho</b>	<b>Tm</b>	<b>Yb</b>	<b>Lu</b>
1998019819	21.00	44.00	88.00	35.00	6.50	1.10	0.60	1.50	0.30	2.30	0.40
1998019847	18.00	48.00	92.00	34.00	6.20	0.90	0.50	0.80	0.20	1.70	0.33
1998019879	28.00	47.00	95.00	37.00	6.80	1.20	0.70	1.20	0.40	2.30	0.42
1998019881	28.00	43.00	86.00	33.00	6.20	1.10	0.60	1.10	0.30	2.40	0.40
<b>Pillow lavas</b>	<b>Y</b>	<b>La</b>	<b>Ce</b>	<b>Nd</b>	<b>Sm</b>	<b>Eu</b>	<b>Tb</b>	<b>Ho</b>	<b>Tm</b>	<b>Yb</b>	<b>Lu</b>
1998019856	19.00	6.80	16.00	8.00	2.90	1.00	0.50	1.00	0.50	2.30	0.32
1998019861	31.00	5.60	14.00	9.00	3.90	1.40	0.80	1.40	0.60	3.20	0.42
<b>Mafic dykes</b>	<b>Y</b>	<b>La</b>	<b>Ce</b>	<b>Nd</b>	<b>Sm</b>	<b>Eu</b>	<b>Tb</b>	<b>Ho</b>	<b>Tm</b>	<b>Yb</b>	<b>Lu</b>
1998019846	13.00	22.00	42.00	18.00	3.20	0.90	0.20	0.50	0.30	1.30	0.14

## **APPENDIX II Microprobe Analysis**

The composition of sulfides and electrum were determined with an automated JEOL-8900L electron microprobe. The standards used were pyrite, chalcopyrite, sphalerite, galena, tetraedrite, arsenopyrite, bismuthinite, and calaverite.

**APPENDIX II**  
**Microprobe Analysis (%)**

**Electrum analysis**

Sample #	61	65	66	69	81	85	91
S	0.40	0.33	0.22	0.20	0.23	0.10	0.07
As	0.00	0.01	0.01	0.00	0.01	0.01	0.00
Fe	1.43	1.15	0.69	0.09	0.28	0.05	0.09
Te	0.12	0.09	0.06	0.09	0.09	0.01	0.05
Ag	26.42	25.19	26.32	30.99	30.02	12.36	14.67
Zn	0.01	0.04	0.00	0.01	0.03	0.00	0.02
Au	70.12	70.29	72.97	67.96	69.86	88.90	86.27
Cu	0.06	0.03	0.00	0.00	0.02	0.02	0.00
Bi	0.21	0.31	0.27	0.47	0.59	0.44	0.49
Total	98.78	97.44	100.54	99.81	101.12	101.89	101.75

**Pyrite analysis**

Sample #	68	70	76	78	80	89	94	97	114	118
S	38.86	37.85	39.01	38.71	39.96	38.06	37.36	37.26	37.71	38.05
As	0.01	0.01	0.02	0.03	0.02	0.01	0.02	0.00	0.03	0.01
Fe	59.72	60.13	60.37	60.26	60.33	59.93	60.24	59.66	60.68	60.16
Te	0.00	0.00	0.01	0.06	0.02	0.00	0.00	0.04	0.04	0.02
Zn	0.00	0.00	0.00	0.00	0.00	0.01	0.01	0.00	0.03	0.00
Au	0.00	0.02	0.00	0.00	0.00	0.00	0.02	0.01	0.02	0.01
Cu	0.05	0.03	0.11	0.03	0.04	0.02	0.00	0.03	0.06	0.06
Hg	0.22	0.24	0.03	0.15	0.03	0.10	0.00	0.13	0.02	0.28
Total	98.88	98.29	99.55	99.24	100.41	98.14	97.65	97.14	98.59	98.58

**Pyrrhotite analysis**

Sample #	62	74
S	52.87	50.59
As	0.01	0.02
Fe	44.13	47.61
Te	0.00	0.05
Zn	0.02	0.01
Au	0.02	0.02
Cu	0.04	0.04
Hg	0.07	0.11
Total	97.18	98.46

**APPENDIX II (CONT'D)**  
**Microprobe Analysis (%)**

**Sphalerite analysis**

Sample #	64	67	71	73	79	82	83	90	105
S	33.14	33.00	32.85	32.77	33.23	33.08	32.75	32.82	31.55
As	0.00	0.00	0.02	0.01	0.00	0.00	0.01	0.01	0.00
Fe	4.54	5.34	9.17	8.97	8.47	8.57	8.15	8.68	8.10
Te	0.01	0.00	0.00	0.00	0.00	0.00	0.00	0.00	0.01
Ag	0.00	0.01	0.00	0.00	0.00	0.01	0.00	0.00	0.00
Zn	64.15	61.30	57.41	58.40	57.51	57.46	58.81	58.16	58.81
Mn	0.01	0.00	0.05	0.05	0.15	0.05	0.07	0.06	0.06
Sb	0.00	0.00	0.00	0.00	0.00	0.00	0.01	0.00	0.00
Cu	0.00	0.00	0.01	0.00	0.00	0.00	0.00	0.72	0.50
Hg	0.07	0.00	0.00	0.02	0.11	0.23	0.08	0.00	0.00
Total	101.92	99.65	99.51	100.22	99.49	99.40	99.88	100.45	99.03

**Chalcopyrite analysis**

Sample #	72	75	77	84	87	88	107	109	111	113	117
S	33.43	34.23	34.26	34.33	33.65	33.53	33.35	33.81	33.78	33.44	32.78
As	0.00	0.00	0.02	0.01	0.03	0.01	0.03	0.02	0.01	0.01	0.01
Fe	30.32	30.57	30.54	30.09	30.35	30.76	30.30	30.22	30.46	30.24	30.55
Te	0.03	0.04	0.00	0.00	0.03	0.00	0.00	0.03	0.02	0.00	0.03
Ag	0.01	0.03	0.04	0.01	0.01	0.02	0.01	0.03	0.02	0.02	0.02
Au	0.00	0.00	0.00	0.00	0.02	0.00	0.00	0.02	0.00	0.02	0.00
Cu	35.58	34.86	35.38	35.57	35.66	35.29	35.65	35.00	36.03	35.48	35.69
Hg	0.15	0.23	0.18	0.01	0.00	0.00	0.10	0.14	0.00	0.00	0.31
Total	99.53	99.97	100.42	100.02	99.75	99.60	99.44	99.28	100.33	99.21	99.40

**Telluro bismuthite analysis**

Sample #	86	92
S	1.27	0.05
As	0.01	0.03
Fe	0.31	0.18
Te	34.11	44.95
Ag	0.00	0.28
Pb	7.64	8.64
Zn	0.04	0.06
Mn	0.00	0.01
Sb	0.24	0.48
Hg	0.10	0.22
Bi	57.03	45.08
Total	100.76	99.97

**APPENDIX II (CONT'D)**  
**Microprobe Analysis (%)**

<b>Galena analysis</b>		
<b>Sample #</b>	<b>96</b>	<b>99</b>
<b>S</b>	12.38	12.57
<b>Fe</b>	0.19	0.39
<b>Te</b>	0.14	0.12
<b>Pb</b>	87.86	88.23
<b>Zn</b>	0.04	0.03
<b>Mn</b>	0.00	0.01
<b>Cu</b>	0.09	0.00
<b>Hg</b>	0.30	0.36
<b>Total</b>	101.00	101.69